



# Modern outlook on the source of the 551 AD tsunamigenic earthquake that struck the Phoenician (Lebanon) coast

Amos Salamon<sup>1,2,3</sup> · Rachid Omira<sup>2,3</sup> · Motti Zohar<sup>4</sup> · Maria Ana Baptista<sup>3,5</sup>

Received: 1 December 2023 / Accepted: 7 March 2024  
© The Author(s) 2024

## Abstract

On July 9th, 551 AD, a strong earthquake followed by a noticeable tsunami and another destructive shock hit the littoral zone of Phoenicia, currently Lebanon. The sequence of events was associated with active faults in the region, but the source able to explain both seismic and tsunami effects is still a matter of open debate. This article contributes to unlocking this enigma by providing a modern analysis of the historical accounts of macroseismic effects, earthquake environmental and tsunami effects, and archaeoseismic findings. Here, we conduct seismotectonic research, evaluate the intensities of all the associated effects, and perform coseismic deformation and numerical tsunami modeling to infer the most likely source. Our results suggest that either the thrust system noted as Mount Lebanon Thrust underlying Lebanon and crops out at the seabed offshore of the coast or the intermittent transpressive Tripoli-Batroun-Jounieh-Damour fault zone along the Lebanese coast are the best candidate sources for the 551 AD earthquakes and tsunami. Both of these sources allow us to better explain the macroseismic, morphological and tsunamigenic effects. Remarkably, the notable uplift of the coastal, marine-cut terraces along the Lebanese littoral zone is well reproduced by the coseismic uplift associated with these sources, thus also clarifying the considerable drawback of the sea and limited inundation reported by the historical accounts.

**Keywords** Beirut · Coseismic deformation · Historic earthquake · Intensity map · Lebanon · Tsunami scenarios

## 1 Introduction

At the tenth hour of the day, Sunday, July 9, 551 AD (551 in short), two successive earthquakes destroyed the major cities along the Phoenician littoral coast of Lebanon (Fig. 1). The region's inhabitants described a sudden retreat and return of the sea, a tsunami in modern terminology, following the earthquake shaking. The concentration of earthquake damage along the coast and the occurrence of an instantaneous "seismic sea wave" led researchers to hypothesize two causative scenarios: an offshore earthquake that generated a tsunami or an inland seismic event that triggered a tsunamigenic submarine landslide. This

dilemma motivated us to decipher the puzzling sequence of events and unravel the responsible sources.

## 1.1 Seismotectonics

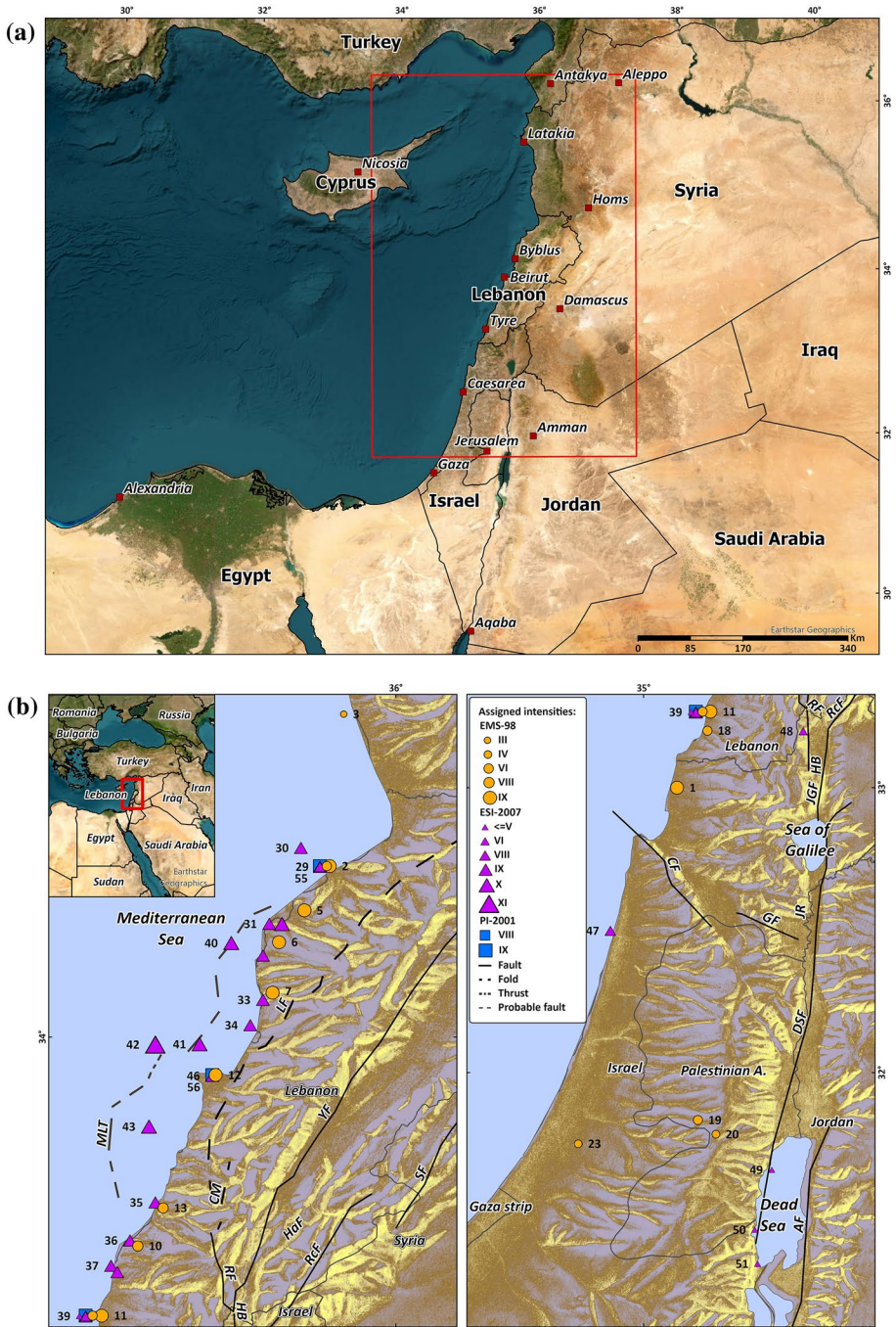
Plate tectonics control the seismic and tsunamigenic activities that affect the Eastern Mediterranean Basin and the Levantine coasts. Here, the Dead Sea Transform (DST), which borders between the Arabian Plate and the Sinai Subplate, is the primary cause of strong earthquakes in the east (e.g., Salamon et al. 2003; Zohar 2020; and references therein). Northward, the Cypriot Arc (CA), which absorbs the collision between the Sinai Subplate and Anatolia, is the main source of sizeable earthquakes (e.g., Wdowinski et al. 2006; Darawcheh et al. 2022).

Although the DST traverses the land along the Levantine coast (Fig. 1), history reveals that tsunamis often follow significant earthquakes originating from this coast; thus, some authors attributed tsunami generation to seismogenic submarine landslides (Salamon et al. 2011 and references therein). Such underwater landslides are not unexpected because fresh sediments accumulate along the Levantine passive margins (e.g., Garfunkel and Almagor 1985; Gvirtzman et al. 2008). In addition, marine faulting in the Eastern Mediterranean Basin and mega earthquakes originating along the Hellenic Subduction Arc (e.g., Papadopoulos et al. 2014) were also responsible for tsunamis that hit the Levantine coast (Salamon et al. 2011; Salamon 2011).

The CA accommodates faster relative plate motion than does the DST and produces a higher rate of seismicity (Salamon et al. 2003; Wdowinski et al. 2006). The number of strong earthquakes generated along the CA is also greater than that generated along the DST, but their damaging effects on the Levantine coast are negligible as the CA is located farther away (Zohar 2020). Specifically, the Latakia Ridge, which is the closest element of the CA to the Lebanese coast (Hall et al. 2005), is ~70 km away from Beirut. Furthermore, historical records of tsunamis generated along the CA show much fewer events (Salamon et al. 2011) than the DST.

While the structure of the southern segments of the DST is relatively simple, left lateral and trans-tensional, the central section, around which the 551 sequence probably occurred, is a complex restraining bend (e.g., Garfunkel 1981; 2014). To the south, the average long-term rate of motion of the DST is approximately 5 mm/year, and since its initiation in the Early Miocene, 17–18 Ma, an offset of approximately 109

**Fig. 1** **a** Location map of the study area. It extends around the Eastern Mediterranean Basin, particularly ► the Phoenician (Lebanon) coast. Additionally, it contains a general outline of the Dead Sea Transform and the Latakia Ridge (Faysal et al. 2023). The black rectangle delineates the area presented in Fig. 1b. **b** The study area (left and right panels are for the northern and northern parts, respectively) and spread of the affected localities and the assigned intensities for each: Macroseismic (EMS-98 degrees denoted by orange circles), Environmental Effects (ESI-2007, by purple triangles) and Tsunami Effects (PI-2001, by blue rectangles). The localities are denoted by individual Id numbers and are presented in full in Supplementary Information 1. Note that the legend presents only the evaluated values. For example, no degree V was assigned to any of the intensity scales; thus, degree V is not present in the legend. The tectonic settings were modified after Daëron et al. (2007); Elias et al. (2007); Garfunkel (2010, 2014); Gomez et al. (2007); Meghraoui (2015); Nemer et al. (2006a, 2006b, 2008); Porat et al. (2009). Abbreviations: AF, Arava fault; CF, Carmel fault; DSF, Dead Sea fault; GF, Gilboa fault; HaF, Hasbaya fault; HB, Hula Basin; JGF, Jordan George fault; LF, Lebanon Flexure; MLT, Mount Lebanon Thrust; RcF, Rachaya splay fault; RF, Roun splay fault; SF, Sergaya splay fault; TBJD: Tripoli-Batroun-Jounieh-Damour Faults zone; YF, Yammounch fault.



km has accumulated (e.g., Quennell 1959; Freund et al. 1970; Garfunkel 2014; Beyth et al. 2018). To compensate for such a large offset, the restraining bend of the DST that stretches along the ~200-km-long Yammounch Fault in the north (Fig. 1b, left) needs to

absorb considerable strain. The strain is distributed throughout an ~100-km-wide zone of deformation on both sides of the Yammouneh Fault (Elias 2006). The deformation is carried out by intensive meso-structures (Hancock and Atiya 1979), a series of major folds and faults that build up a mega-anticline, and considerable uplift and exposure of Jurassic formations thrust as high as 2.5 km above sea level (e.g., Dubertret 1955; Walley 1988, 1998; Gomez et al. 2006). Most important with respect to the present study, however, is the complex fault system that seems to include the possible seismogenic source of the 551 earthquake.

The DST has developed across preceding upper Cretaceous and upper Paleogene phases of shortening, known as the Syrian Arc Folds and Faults Belt (Krenkel 1924). Thus, the final outcome, the Mount Lebanon mega-anticline, is a superposition of these two tectonic phases (e.g., Elias 2006). Lebanon of today is stretched, more or less, along this mega-anticline and consequently is strongly affected by its seismotectonic environment. This is evident in the numerous earthquakes recorded throughout geological history. For example, paleoseismic investigations have identified considerable surface ruptures across the whole length of the DST (summary by Marco and Klinger 2014) as well as along most of the major faults associated with the Yammouneh restraining bend (e.g., Gomez et al. 2003; Daëron et al. 2004a; 2007; Nemer and Meghraoui 2006a, b; Nemer et al. 2008). Archaeoseismology revealed sites and structures damaged by strong ground shaking at the time (e.g., Marco 2008 and references therein). Historical accounts have reported frequent earthquakes and tsunamis that destroyed numerous settlements and affected vast regions (Zohar 2020; Salamon et al. 2011), and modern seismicity shows ongoing activity throughout the region (e.g., Brax et al. 2019; Wetzler et al. 2022). As the present plate tectonics configuration is still active (Gomez et al. 2007, 2020; Hamiel and Piatibratova 2021), ongoing seismotectonic activity (Huijjer et al. 2016; Nemer et al. 2023; Salamon et al. 2003) that can generate destructive earthquakes in the region continues. Furthermore, offshore currents have been mobilizing sediments from the Nile Delta northeastwards along the southern Levantine coast (Zviely et al. 2007; Zucker et al. 2021), and river loads originating along the Mount Lebanon range are piling up offshore Lebanon (Elias 2006). As a result, strong seismic shaking can trigger submarine landslides that in turn can generate sizable tsunamis.

Although rare, the 551 sequence exemplifies this process and is without exception. However, retracing the earthquake mechanism is crucial for future earthquake and tsunami hazard evaluations (Huijjer et al. 2016). The present investigation aims to contribute to the assessment of these hazards in the area.

## 1.2 Tsunamis that affected the levantine coasts and their probable sources

Several events involving abnormal sea waves along the Levantine coast that were associated with earthquakes have been reported throughout history. Salamon et al. (2011, and references therein) conducted a critical evaluation of these records and constructed a list of those events—tsunamis—in modern terms. Based on Salamon et al. (2011), we list here (Table 1) the tsunamis that affected the Lebanese coasts. The events that hit the nearby coasts of Syria in the north and Israel in the south are also noted because they may have affected the Lebanese coast as well, but no accounts were left or survived the time. East Mediterranean basin-wide tsunamis are also listed. Thus, it is clear that the

**Table 1** Historical tsunami that affected the Lebanese and nearby coasts. The list is modified after Salamon et al. (2011, and full referencing in there)

Tsunami event	Effects along coasts, cities and harbors	Damage in coastal cities and harbors	Reported loss of lives	Possible earthquake source
1365 ± 5 BC		Ugarit half destroyed		Not mentioned
Mid second century BC	High wave between Tyre and Acre	Caesarea?	People were engulfed and drowned	Not known
13th December 115 AD		Nile delta, Alexandria	Nile delta, Alexandria	DST, Missyaf segment in Syria
* 21st July 365 AD	Sea withdrew and retreated	In Phoenician cities, Beirut	In Phoenician cities, Beirut	Hellenic Arc, Southwest of Crete
9th July 551 AD	Waves rose up to the sky	Most of the cities and villages destroyed		Offshore Lebanon
18th January 746 AD				DST, Jordan Valley
5th December 1033 AD (4th January 1034 AD?)	Water in Acre receded for an hour			DST, Jordan Valley
29th May 1068 AD	In Palestine, sea withdrew and flowed back		Many people were drowned	Not known
20th May 1202 AD	Gigantic waves rose up between Cyprus and Syria	Serious damage to lighthouses, ships were thrown on shore	+	DST, Yammouneh Fault
* 8th August 1303 AD	Sea receded and flooded Acre		People who went to pick objects in the sea were swept away and drowned	Hellenic Arc, Southeast of Crete
29th December 1408 AD	High tide stretched in western Syria	Boats were pushed onto the land, but nothing proved to have been damaged		Northern DST, Hacıpasa and Amik Basin
30th October 1759 AD	Sea wave flooded Acre, and docks at Tripoli	No apparent damage		Rachaiya fault, southwestern Syria
25th November 1759 AD	Sea wave noted as far as the Nile delta	In Acre, ships were thrown onto the shore, no damage in the Nile Delta	Some casualties in Acre	Serghaya fault, southwestern Syria
3rd April 1872 AD	Sea flooded the coasts of western Syria			Northern DST, Hacıpasa segment

\*East Mediterranean basin-wide tsunamis, not specifically reported in Lebanon

Lebanese and neighboring coasts are exposed to tsunami hazards due to both local and regional earthquakes.

### 1.3 The 551 earthquake and tsunami according to historical reports and modern studies

The 551 sequence has attracted the attention of many historians and catalogers. The first group collected and assembled a wealth of information but unfortunately was unaware of hidden mistakes, ambiguous information and duplicated events. Recent researchers, however, realized these shortcomings, closely followed the chain of referencing and transferring information, scrutinized and verified the data, and provided reliable assessments (e.g., Karcz 2004; Guidoboni and Comastri 2005; Ambraseys 2009). Therefore, we base our investigation on the thorough critiques and analyses that presented and interpreted the historical sources and summarized the 551 sequence of events. In case modern researchers published several consecutive papers on the same subject, we refer to the most updated publication, assuming that this is the revised version. Specifically, we referred to the catalogs of Guidoboni et al. (1994), Ambraseys (2009) and Williams (2023) and the focused studies of Darawcheh et al. (2000), Elias (2006) and Elias et al. (2007). Ambraseys (2009) provided a comprehensive description:

*... Damage extended along 100 km of the littoral of Galilee and Phoenice Maritima, where towns and villages on the coast were ruined by two successive earthquakes and the seismic sea wave that followed the first quake. In places, the names of which are not given, the shocks caused the ground to open up and elsewhere they triggered landslides. It is said that 101 towns/villages were affected. Beirut seems to have been the worst hit. It was badly damaged by the earthquake and a sea wave, but most of the destruction seems to have resulted from the ensuing fire, which apparently raged for two months. Buildings and works of art were lost.*

Later overviews included 551 events within the perspective of earthquake and tsunami hazards in the Levantine region (Salamon et al. 2011; Zohar 2020).

Modern studies have expanded the research on the 551 sequence. Sanlaville et al. (1997) and Morhange et al. (2006, Table 1) identified, measured and C14 dated the ~80 cm uplifted marine-cut terraces along the Lebanese coast, and related the uplift to the coseismic deformation induced by the 551 earthquake. Consequently, they suggested an offshore source for this event. Elias (2006) conducted a comprehensive study on the active thrusting associated with the Mount Lebanon mega-anticline, which is centered on the Yammouneh restraining bend, including the tectonics of offshore Lebanon. Daëron et al. (2004a), Elias (2006) and Elias et al. (2007) assessed the SHALIMAR marine mapping and geophysical survey (Singh 2003) and identified fresh sea-bottom scars offshore Lebanon. In their opinion, these scars are surface ruptures of the 551 earthquake generated by the Mount Lebanon Thrust (MLT, also termed the Offshore Monocline by Nemer et al. 2006a, 2006b), which is an integral element of the western flank of the Mount Lebanon mega-anticline. Elias (2006, Fig. 4–2 in there) presented the role of the MLT on a synthetic deep crustal section of Mount Lebanon and its reactivated margin on the basis of a seismic profile offshore Lebanon and geological cross-sections on both sides of the Mount Lebanon range. Elias (2006, Fig. 1-45 in there) also suggested that Ras-Chakka (Chekkaa, Chakaa, Chaka) was the probable location of the subaerial landslides reported by contemporaneous sources in Lithoprosopon. Recently,

Faysal et al. (2023) stated that they “*were not able to confirm the existence of Mount Lebanon thrust using seismic profile data...*”, and suggested that the Latakia Ridge triggered the 551 earthquake and tsunami.

An overview of archaeoseismic findings, whether related to the 551 earthquake or not, is given by Williams (2023). We focused on Marriner et al. (2008, and references therein), who conducted extensive geoarchaeological investigations in the area of the ancient harbor of Beirut and integrated a wealth of information from previous studies. They unearthed and discovered unique findings dated to the Byzantine and later periods. A notable finding is the transition from fine-grained to coarser-grained sediments, which is usually associated with a partial or total abandonment of harbors and/or economic and political decline. They also uncovered sea-scoured bedrock that can be attributed to erosion due to strong tsunami currents. In addition, they noted the spread of ruins, the relative absence of seaport infrastructure, partial abandonment, and limited rebuilding across the city area of Beirut at that time. Furthermore, these authors were able to reconstruct the location of the Romano-Byzantine harbor coastline of Beirut at the time of the earthquake (Fig. 11 dashed blue line, in Marriner et al. 2008). They also inferred that westward and eastward, the harbor coastline appeared to merge with the pre-1840 coastline, which has not changed much since antiquity. Overall, Marriner et al. (2008) concluded that these discoveries echo a catastrophic event, most likely the 551 earthquake and tsunami.

Southward, Goodman-Tchernov et al. (2009) investigated several drill cores offshore of Caesarea, Israel. They interpreted some of the sedimentary deposits as tsunamigenic indicators and suggested that one of them corresponds chronologically to the 551 event. Further study by Dey et al. (2014) suggested a possible mixture of tsunamites originating from the 551 and 749 AD events that hit Caesarea.

In an interdisciplinary study based on texts, archaeological findings and scientific studies, Mordechai (2019) assessed the social, cultural, economic and demographic effects of the 551 earthquake on Berytus (Beirut currently).

The relatively wealth of contemporaneous information collected thus far for the 551 sequence of events contains macroseismic, environmental (a term proposed by Michetti et al. 2004 for seismically induced ground effects in the natural environment) and tsunami effects. These are essential for studying the seismogenic and tsunamigenic sources of the 551 events, which is the purpose of our work.

## 1.4 Sources proposed for the 551 earthquakes and tsunami

Identifying the source of historical earthquakes is challenging due to a lack of instrumental data. Instead, the research is based on the spread of macroseismic and archaeoseismic damage and environmental effects. However, if the reported damage and effects extend along linear coastal zones, it is almost impossible to determine whether the source was on- or offshore. Moreover, in the case of tsunami generation, the possibility of an inland earthquake triggering a tsunamigenic submarine landslide cannot be ruled out. Furthermore, while earthquake and tsunami simulations require knowledge of the source parameters and mechanism, historical accounts mention only the affected localities. In addition, some early modern studies interpreted seismogenic and tsunamigenic generators as point sources and provided vague descriptions, such as ‘offshore fault’, and seldom delineated the fault trace.

For the 551 earthquake and tsunami, the concentration of the reported damage along the Lebanese littoral and the absence of damage accounts from inland Lebanon led researchers to assume an offshore source (e.g., Guidoboni et al. 1994). On the other hand, the presence of

considerable submarine landslides offshore of the Levantine coast (Katz et al. 2015, and references therein) and a wealth of paleoseismic evidence of historical earthquakes inland (Marco and Klinger 2014) suggest that onshore earthquakes may have triggered tsunamigenic submarine landslides and that the 551 sequence could have been such a case as well. Ambraseys (2009) discussed the 551 epicenter dilemma: "... either offshore, off Lebanon and Syria, or, which is the most likely possibility, inland not far from the coast".

Darawcheh et al. (2000) suggested that the earthquake resulted from an on-land, left-lateral strike-slip mechanism on the Roum fault with a magnitude range of Ms 7.1–7.3 but located the epicenter offshore of Beirut. Indeed, the Roum Fault bifurcates on land from the DST in southern Lebanon and strikes toward Beirut, but according to geological (Dubertret 1955) and structural (Walley et al. 1998) maps, it fades well south of Beirut and does not intrude the sea. Furthermore, the paleoseismic study of Nemer and Meghraoui (2006a, b) favored the Roum Fault as the source of the 1837 event. This is also in accord with the extensive spread of damage in southern Lebanon and northern Israel, rather than the 551 event that mostly affected the Lebanese coast. Recent studies by Daëron et al. (2004b), Elias (2006) and Elias et al. (2007), however, suggested the offshore MLT as the source of the 551 earthquake on the basis of the local geology and marine bathymetry survey and proposed a magnitude range of Mw 7.4–7.6. In addition, Elias et al. (2007) examined the SHALIMAR bathymetry survey (Singh 2003) and found a limited volume of fresh mobilized sediments offshore Lebanon. Thus, they questioned the contribution of a submarine landslide to 551 tsunami generation. Recent investigations of the framework of geological faults offshore Lebanon by Faysal et al. (2023) challenged the role of the MLT and instead proposed the Latakia Ridge, the southeasternmost segment of the CA, as the seismotectonic origin of the 551 earthquake and tsunami. However, they still raised the need to verify the absence of the MLT by "... further investigation on high resolution, deep seismic reflection data that cover both the offshore and onshore areas".

Two additional sources are worth mentioning. The first one was proposed by modern researchers but was later noted to be erroneous by critic catalogs. Ambraseys et al. (1997) suggested a source of M7.5 in Trans Jordan (east of the Jordan River) several tens of kilometers northeast of the Dead Sea, and this source was subsequently adopted by Migowski et al. (2004). However, Ambraseys (2009) explained that "Ambraseys et al. (1997, 24–25) wrongly place the epicentral region of this event in the Jordan Rift Valley [...] due to the bias of information from the debatable archaeological evidence in Russell (1985)". The second source is Ben Menahem (1991), who suggested an M7.5 source in the northern Corinthian Gulf (N38.4, E22.3), but according to Guidoboni et al. (1994) and Ambraseys (2009), Ben Menahem amalgamated the 551 event of Lebanon with another earthquake and tsunami that occurred nearly at the same time and affected Kos town (N36°53' E27°17') in the Aegean Sea.

Subaerial landslide tsunami along the Levantine coast was mentioned in association with the December 29, 1408 strong earthquake inland of western Syria, possibly due to the collapse of Mt. Cassius (Ambraseys 2009). Interestingly, however, no exceptional waves were mentioned by contemporaneous sources in association with the subaerial landslide in Lithoprosperon during the 551 events, despite the presence of submarine sediments offshore Ras-Chakka (which, according to Elias (2006), was called Lithoprosperon at the time). Thus, this tsunamigenic source can be ruled out.

## 2 Goal and methodology

Here, we join the ongoing discussion on the potential 551 earthquake and tsunami sources. The discrepancies among the abovementioned sources need testing to verify whether they conform to the documentary data and the discovered evidence. In addition, we examine the seemingly contradictory descriptions of the significant retreat of the sea and the limited inundation, as was described by the historical account “... *the sea return to its original level*” (Ambraseys 2009). We thus framed our investigation as follows:

- Database preparation and synthesis (Sect. 3)
  - Search, collect and construct a database of macroseismic, tsunami and environmental effects from documentary data, geomorphological, and geoarchaeological studies, and marine surveys;
  - Assign intensity degrees to the assembled effects;
  - Identify the potential seismogenic and tsunamigenic sources proposed by previous researchers for the 551 events and define their source parameters;
  - Assemble bathymetry and topography grid and reconstruct Beirut paleo-coastline at the time of the 551 events.
  
- Modeling and simulation (Sect. 4)
  - Construct iso-seismal map of the 551 event on the base of the intensities assigned to its various effects;
  - Compute the coseismic deformation (Okada 1985) of the proposed sources. Here, Okada’s (1985) half-space elastic deformation theory is used to simulate the static vertical dislocation produced by the rupture of each 551-like earthquake scenario. The derived rupture fault parameters (i.e., location, dimensions, dip, rake, strike and slip) form the input for Okada’s model;
  - Select the most favorable earthquake source that best explains the spread of earthquake effects, including the uplifted marine-cut terraces. This source can also be a tsunamigenic source.;
  - Simulate the tsunami generation and wave propagation according to the proposed tsunamigenic sources. The tsunami initial wave is derived by transferring the simulated coseismic deformation to the free sea surface with the assumption that the sea disturbance mimics the seafloor deformation. This initial wave is then propagated using a validated nonlinear shallow water equations code;
  - Produce time series of the tsunami waves at selected locations along the Beirut coast. This approach involves simulating synthetic tsunami waveforms to analyze the temporal evolution of tsunamis in offshore coastal areas;
  - Select the most favorable tsunamigenic source that best explains the reported tsunami effects. The obtained simulation results (coastal uplift, leading wave, wave height, etc.) are directly compared with the available reports, evidence and observations to help infer the best candidate source for the 551 event.
  
- Discussion (Sect. 5)

- Discuss the computed earthquake and tsunami scenarios against the suite of reported damage and effects, and identify the most favorable sources among the previously suggested ones;
  - Discuss the effect of coseismic uplift or subsidence on tsunami inundation and its implications for earthquake and tsunami hazard assessments;
  - Discuss unresolved gaps and open questions.
- Summary and Conclusions (Sects. 6 and 7)
    - Summarize the project and key findings
    - Identify the most favorable and reasonable earthquake and tsunami generators for the previously proposed sources.
    - Propose avenues for future research

### 3 Database preparation and synthesis

Recent developments enable combining different intensity scales under the same umbrella, namely, the EMS-98 macroseismic (Grünthal 1998), the PI-2001 tsunami (Papadopoulos and Imamura 2001) and the ESI-2007 environmental (Serva et al. 2016) effects. These scales comprise 12 grades that are generally in line with each other. Thus, assembling and integrating the available documentary data and field evidence of the 551 events allows us to construct an isoseismal map that may constrain the 551 earthquake and tsunami source and reject sources that do not conform to the actual evidence.

Previous studies have already graded macroseismic intensities with respect to documentary data and effects. However, as this process is subjective and depends on expert judgment (e.g., Musson and Cčić 2012), we favored consistent assessment of our database. To do this, we used the abovementioned three different independent intensity scales and reevaluated the grades. Interestingly, we found that several of the 551 tsunami effects have the same intensity values at the PI-2001 and ESI-2007 scales.

The historical documentary data mention two successive earthquakes and a tsunami in between but do not resolve or differentiate the effects and severity of damage among them and of the ensuing fire. Intuitively, since the tsunami followed the first earthquake, this was considered the main shock, and the second tremor was considered the aftershock. However, the impact of the second earthquake, as described in Beirut, suggested that it might have also been destructive (Guidoboni et al. 1994, and references in there, translated John of Ephesus who probably quoted the historians Malalas: “*As the sea was rising up against them from behind, the earthquake brought down the city in front of them*”). One can speculate that the second shock was as strong as the first quake, if not stronger and tsunamigenic. Nevertheless, distinguishing the scope and severity of damage caused onshore by the two earthquakes and the tsunami remains impossible. Some reports describe the spread of damage and effects along linear or areal zones rather than specific localities and name the zone by its contemporaneous geography. Here, we refer to historical places by their modern names and the location of their oldest sector.

Naturally, the available historical sources might be inaccurate, unreliable, or exaggerated (Guidoboni and Ebel 2009). Thus, the spread of damage and effects cannot be considered complete, and evaluating their severity is occasionally a complex task. Consequently,

to mitigate potential erroneous interpretations due to the inherent shortcomings of historical reports, it is necessary to consider the contemporaneous nature of the sources (see further discussion in Zohar et al. 2016).

Given the problems of historical information and the association of environmental effects with specific past events, we also discuss the reliability and uncertainty of the data. In our case, we favored contemporary (primary) sources over secondary sources. Damage or effect that was reported by two independent contemporary or near-contemporary sources was considered reliable, while a single secondary source that draws from a questionable earlier secondary source was considered doubtful or rejected.

### 3.1 Macroseismic effects

The macroseismic effects that were found to be relevant to the 551 event and quantifiable by the EMS-98 Intensity Scale are summarized in Table 2. The Table lists each of the affected localities and their geographic coordinates; the most severe effects reported for the given site and the EMS-98 intensity degree we have assigned it; estimated reliability and uncertainties; and comments that brief the effect. All the information and descriptions that are presented in Table 2 were taken from the comprehensive reviews of Guidoboni et al. (1994) and Ambraseys (2009), which we consider highly reliable because they have conducted careful screening of the historical accounts. Both the reliability and uncertainty of the assigned EMS-98 intensities were considered high (H) for specific localities and moderate (M) if related to a general geographic area. The “no information” from neighboring territories was considered poor (P), where likely there was no effect at all, or nobody to report from there or that the report is lost, etc. Poor reliability data, however, were rejected.

Given the typical building materials along the Lebanese littoral and western foothills of Mount Lebanon (Gwiazda and Waliszewski 2014), which are rubble stone, fieldstone and simple stone and wood, the local structures are considered type A and B vulnerabilities (see the EMS-98 definition by Grünthal, 1998). The scope of damage presented by Ambraseys (2009), who translated the documentary data, is described as “... *many cities of the Phoenician littoral collapsed... of the surrounding villages 101 fell, ... multitudes of men were crushed in these cities... completely razed to the ground and their inhabitants all killed*”. The EMS-98 classifies such levels of damage to masonry buildings as grades 4 and 5 and considers a minimal intensity degree of IX (Destructive). Table 2 summarizes the evaluation of all the available macroseismic effects related to the 551 earthquake.

### 3.2 Tsunami effects

The historical reports of the 551 exceptional sea waves focused on what had happened in Beirut harbor and the nearest offshore area. Descriptions of effects elsewhere along the Phoenician (Lebanon) coast were vague. Moreover, the terminology of the geography of the affected area differs among modern researchers, from “*the Syrian coast*” (Ambraseys 1962) to “*the coast of Phoenice*” (Ambraseys et al. 1997), “*the Lebanese coast*” (Amiran et al. 1994), and “*between Tyre and Tripoli*” (Darawchek et al. 2000, regarding coastal cities). This information is important for accurately delineating the extent of the affected coast at the time in terms of modern geography. Unfortunately, even the descriptions of the coastal extent of Lebanese Phoenicia, whether Tyre, Acre or Dor was its southernmost city, are not certain. Here, we follow the stretch of the affected coastal area as determined by the latest available studies, namely, Darawchek et al. (2000) and Ambraseys (2009). Other

**Table 2** EMS-98 macroseismic intensities assigned to localities affected by the 551 earthquakes

Location (synonym/ms)	Coordinates Lat. N—Long. E	Effects/Damage	EMS-98 Intensity	Reliability, uncertainty	Comments
Along the littoral of Galilee and Phoenice Maritima (i.e. Tripoli to Acre)	Central Galilee littoral: 33°00' 35°05' Tripoli: 34°27' 35°48'	"Towns and villages on the coast were ruined by two successive earthquakes"	≥ IX	M	General description
Aradus Island (Antharidus, Arwad)	Arwad: 34°51' 35°51'	Aradus—probably felt	≥ III	H	Many people were killed; "many cities of the Phoenician littoral collapsed, ... and multitudes of men were crushed in these cities... with their livestock and everything else"
Tripolis	Tripoli: 34°27' 35°48'	Tripoli—collapsed	≥ IX	H	
Trieris (Shikka, Shaqa)	Shaqa: 34°20' 35°44'	Shaqa—ruined, collapsed	≥ IX	H	
Botrys (Batroun)	Batroun: 34°15' 35°40'	Batroun—collapsed	≥ IX	H	
Byblus	Byblus: 34°07' 35°39'	Byblus—collapsed	≥ IX	H	
Berytus (Beirut)	Beirut: 33°54' 35°30'	Beirut—ruined	≥ IX	H	
Sidon	Sidon: 33°33' 35°22'	Sidon—ruined in part	≥ VII-VIII	H	
Sarepta (Sarfand)	Sarfand: 33°27' 35°18'	Sarfand—ruined in part?	≥ VII-VIII	H	
Tyros (Troy, Tyro, Sur)	Tyr: 33°16' 35°12'	Tyr—ruined	≥ IX	H	
Beirut	33°54' 35°30'	Worst hit and badly damaged by the earthquake and a sea wave; At least 30 000 people died in Beirut	≥ IX	H	Beirut was a central hub, thus the damage is more detailed and may appear worse than elsewhere. The ensuing fire increased the damage and confuses intensity evaluation
Sidon	33°33' 35°22'	"...which cannot therefore have been badly damaged..." i.e. ruined in part	≥ VII-VIII	H	
101 towns/villages in Lebanon (assumed between Tyre and Tripoli)	Tyre: 33°16' 35°11' Tripoli: 34°27' 35°48'	Were affected	≥ VI	M	Around the affected littoral cities, but no mention of the exact location
Between Laodicea and Antioch	Laodicea 35°32' 35°47' Antioch 36°12' 36°22'	Everything except "a few towers of city walls, and church walls" remained standing and the southern region were likewise preserved"	≥ VI	H	
From south of Tyre to north of Jerusalem	Tyre: 33°12' 35°12' Jerusalem: 31°50' 35°10'	"There is no evidence that Jerusalem was affected"	≥ VI	H	
Jerusalem	31°47' 35°14'		–	P	Intensity degree cannot be determined

**Table 2** (continued)

Location (synonyms)	Coordinates Lat. N—Long. E	Effects/Damage	EMS-98 Intensity	Reliability, uncertainty	Comments
<i>“Then in Alexandria the Great too, which is situated on the River Nile, a place unaccustomed to earthquakes”</i>	31°12' 29°53'	<i>“A very slight tremor was perceived, although it was very weak and not widely felt.”</i>	III	H	
Antioch:	36°12' 36°22'	Felt	≥ III	H	The coordinates relate to the assumed region
Palestine:	31°45' 34°45'				
Arabia (East of the Jordan River):	31°45' 35°50'				
Mesopotamia:	34°30' 42°30'				
Cyprus, Rhodes, the hinterland to the north and the east		<i>“It is rather strange that there is no information from Cyprus, Rhodes and, in particular, the hinterland to the north and the east, where the earthquake should have been quite strong”</i>	–	P	No information: may be interpreted as intensity I, or just lack of data which means that intensity degree cannot be determined

The locations as well as the damage descriptions and effects are based on the interpretations of Ambraseys (2009, pp. 199–203) and Guidoboni et al. (1994, pp. 332–336). Quotations, presented in italics, are from Ambraseys (2009)

tsunami effects, identified in Beirut by geoarchaeological investigation (Curvers and Stuart 2004) and offshore Caesarea by fieldwork (Goodman-Tchernov et al. 2009; Dey et al. 2014; Goodman-Tchernov and Austin 2015), were also linked to the 551 event.

Table 3 lists the tsunami effects relevant to our analysis and assessable by the PI-2001 Intensity Scale (Papadopoulos and Imamura 2001). The data refer to the affected coast and its geographic coordinates, the assigned PI-2001 intensity degree, and the estimated reliability and uncertainties. The last column, “comments and references”, briefly describes the effect and refers to its source. The reliability and uncertainty of the data related to specific localities were defined as high (H), and the information given for geographic areas in general was defined as moderate (M). Geoarchaeological and assumed tsunamite left marks were considered low (L) due to the large timeframe and uncertainty in age determination.

### 3.3 Environmental effects

Aside from the tsunami effects and the subaerial landslide in Lithoprosopon (Ras-Chakka, near the Botrys coast of today) mentioned by historical accounts, modern researchers associated additional environmental effects with the 551 earthquake. A series of uplifted marine-cut terraces along the Phoenician coast, from Tyre to Tripoli, were identified and <sup>14</sup>C dated by Sanlaville et al. (1997) and Morhange et al. (2006, Table 1 in there). In their study, the uplift, approximately 80 cm along 100 km of the Lebanese littoral zone, was most likely induced by the coseismic deformation of the 551 earthquake. These findings were then adopted by Elias (2006) and Elias et al. (2007), linked with seafloor breaks offshore Lebanon, and interpreted as surface ruptures of the MLT during the 551 earthquake. In our opinion, these breaks are environmental effects as well.

Kagan et al. (2011) identified and dated seismites in three stratigraphic sections (Ein Feshkha, Ze'elim and Ein Gedi) along the western shores of the Dead Sea and associated some of them with the 551 earthquake, albeit with some range of uncertainty. Further discussion on these findings is presented by Williams (2023). Kanari et al. (2019) examined and dated rockfalls in Qiryat-Shemona, northern Israel, and attributed the failure to historical earthquakes, possibly the 363 and/or 502 or 551 AD.

We note that all the tsunami, tsunamite and scouring effects considered here as environmental effects (Table 4) were also listed as tsunami effects (Table 3). They were examined independently by both tsunami and environmental intensity scales, resulting in the same intensity degrees (Tables 3, 4). However, for the iso-seismal analysis (Sect. 4.1), they were considered and weighed only once.

In line with the reliability and uncertainties afore-defined, we assigned high (H) to data related to specific localities and low (L) to data related to effects associated with the 551 event with a large timeframe in age determination. Faysal et al. (2023) attributed the bathymetry scarps off coast Lebanon to local, surficial salt tectonics rather than seismotectonic rupture of the MLT, as suggested by Elias et al. (2007). We thus assigned low (L) reliability to these effects.

### 3.4 Potential seismogenic sources

The discussion of the possible sources of the 551 earthquake revealed two directions, inland and offshore, whereas recent researchers tend toward the latter option (see Sect. 1.3). Most notably, the MLT offshore Lebanon is capable of triggering 7.4–7.6 Mw earthquakes (Elias 2006; and Elias et al. 2007). A recent seismic hazard assessment in

**Table 3** Intensity degrees assigned to tsunami effects related to the 551 event according to the Papadopoulos and Imamura (2001) tsunami intensity scale

Location	Coordinates Lat. N—Long. E	Effect	PL-2001 Intensity	Reliability, uncertainty	Comments and references
Phoenicia coast (Tyre to Tripoli)	Tyre: 33° 16' 35" 11' Tripoli: 34° 27' 35" 48'	Tsunami	≥ VIII	M	<i>"The sea receded for many hours by one to two miles... Then the sea came back"</i>
All Phoenician Coast, or just in Beirut	Tyre: 33° 16' 35" 11' Tripoli: 34° 27' 35" 48', Or Old Beirut: 33° 54' 35" 31'	Casualties: 30,000 people were drowned...	≥ IX	M	<i>"...a grossly exaggerated figure given for Beirut alone"</i>
Ancient Beirut harbor	33° 54' 35" 31'	<i>"Then the sea came back, throwing ships on land, causing great havoc before returning to its original level"</i>	≥ IX	H	Evaluation of historical accounts (e.g. Elias 2006; Ambraseys 2009; and others)
Ancient Beirut harbor	33° 54' 35" 31'	Scouring (Marriner et al. 2008): <i>"Surveys in the Ottoman harbour have unearthed harbour muds and silts which lie unconformably above sea-scoured bedrock... These have been attributed to tsunami action and indirectly infer considerable damage to the city's seaport infrastructure"</i>	≥ IX	L	Marriner et al. (2008) after Curvers and Stuart (2004)
Caesarea	~ 34° 30' ~ 34° 53'	Tsunamiite, assumed	≥ VIII	L	Goodman-Tchernov et al. (2009), Dey et al. (2014)

Quotations are presented in italics, and except if otherwise mentioned, they were taken from Ambraseys (2009)

**Table 4** Intensity degrees assigned to environmental effects associated with the 551 event according to the ESI-2007 Scale (Serva et al. 2016)

Location	Coordinates Lat. N—Long. E	Environmental effect	ESI-2007 Intensity	Reliability	Comments
Lithoprosopon (Ras al-Shaqqaq), Botrys coast	~34° 18' ~35° 42'	Subaerial landslide	X	H	Evaluation of historical accounts (e.g. Elias 2006; Ambraseys 2009; and others)
Not specified, but is inferred to be around the damaged area between Tripoli to Tyre	Tyre: 33° 16' 35" 11' Tripoli: 34° 27' 35" 48'	Ambraseys (2009): "... the mountains were uprooted and cloven with force; and fissures opened in the ground in diverse places"	≥ VIII	H	By association and elimination, the affected area is around the damaged area
Qiryat-Shemona	33° 12' 35" 34'	Rockfalls, Volume of 25–41 M <sup>3</sup>	≥ VI	L	Kamari et al. (2019): "... we cannot completely rule out the possibility that these were two separate rockfall events, both triggered by large earthquakes in 363 and 502/551 CE."
Western coast of the Dead Sea	Ein Feshkha: 31° 40' 35" 27' Ein Gedi: 31° 27' 35" 23' 30" Ze' elim Gully: 31° 20' 35" 24'	Seismites	≥ V	L	Kagan et al. (2011) associated seismites in these field cross sections to the 551 earthquake
Uplifted marine-cut terraces along the Phoenicia coast from Tyre to Tripoli Data from Morhange et al. (2006, Table 1), Sanlaville et al. (1997), adopted by Elias (2006) and Elias et al (2007)					
Location	Coordinates Lat. N—Long. E	Range of Uplift (rounded, in cm)	ESI-2007 Intensity	Reliability	Comments
Tripoli Islands	~34° 30' ~35° 45'	60–110	IX	L	
Hannouch, Near the promontory of Ras Chekka	~34° 18' ~35° 40'	0/20–60	IX	L	
Madfoun	34° 13' 35" 39'	80–110	IX	L	
Fidar	34° 06' 35" 39'	50	IX	L	
Tabarja	34° 02' 35" 37'	50–120	IX	L	
Saida	33° 34' 35" 22'	50	IX	L	
Ras Qantara	33° 28' 35" 18'	50	IX	L	

**Table 4** (continued)

Location	Coordinates Lat. N—Long. E	Environmental effect	ESI-2007 Intensity	Reliability	Comments
Ras Abou Zeid	33°24' 35°15'	70	IX	L	
Khaizerane	~33°23' ~35°16'	40	IX	L	
Tyre	~33°16' ~35°10'	0	I	L	
Selected submarine surface rupture locations, from Elias (2006)					
Offshore Batroun	~34°15' ~35°34'	Length: ~3 km	X	L	
Offshore Jounieh	~33°59' ~35°29'	Length: ~3 km	X	L	
Offshore Beirut	~33°59' ~35°22'	Length: ~20 km	XI	L	
Offshore Damour	~33°46' ~35°21'	Length: ~4 km	X	L	
The following effects were evaluated also by Tsunami Intensity Scale (Table 3)					
Phoenicia coast: Tyre to Tripoli	Tyre: 33°16' 35°11' Tripoli: 34°27' 35°48'	Tsunami	≥ IX	H	The coast in between Tyre and Tripoli
Ancient Beirut harbor	33°54' 35°31'	Scouring (see Table 3)	≥ IX	L	Marriner et al. (2008) after Curvers and Stuart (2004)
Caesarea	~34°30' ~34°53'	Tsunamite, assumed	≥ VIII	L	Goodman-Tchernov et al. (2009), Dey et al. (2014)

Lebanon by Nemer et al. (2023) also considered this structure to be a potential 551 tsunami-generating source. On the other hand, Faysal et al. (2023) challenge the role of the MLT and suggested that the active transpressive fault system beneath the Latakia Ridge (Fig. 1a) was a plausible source of the 551 earthquake and tsunami. Although they did not find a major thrust system offshore Lebanon, they attributed the uplift of the coastal regions to the intermittent transpressive Tripoli-Batroun-Jounieh-Damour(TBJD) fault zone. In our opinion, the TBJD is a more plausible seismogenic source of the 551 earthquake and tsunami than the transtension/pression Latakia Ridge because the former is approximately 10–20 km away from the Lebanese margins and the latter is about 70 km away. In that sense, our computed earthquake and tsunami scenarios represent both the MLT (after Elias et al. 2007) and the TBJD (after Faysal et al. 2023).

Previously, Darawcheh et al. (2000) proposed an Ms7.2 earthquake on the Roum fault, inland southern Lebanon, as the 551 source; however, for some reason, they placed its epicenter offshore of Beirut. Wechsler et al. (2014) investigated paleoseismic events in Bet-Zayda, along the Jordan Gorge Fault, just north of the Sea of Galilee, and suspected that the 551 earthquake could have been one of them. Williams (2023) joined the discussion and proposed that “... the 551 C.E. earthquake is thought to have ruptured offshore Lebanon, on the Mount Lebanon Thrust (Elias et al. 2007). Yet we must consider the possibility that the rupture extended to the south, along the Roum fault (Darawcheh et al. 2000) and onto the JGF (Wechsler et al. 2009) or that what is described as one earthquake in the historical record was actually a series of events, one triggering the other, that were amalgamated in the historical record”.

In Ambraseys’ (2009) opinion, “It is equally possible, however, that the earthquake was on-land, on the Roum or Mammounieh faults, from where the shock could have easily triggered an offshore submarine slide, which in turn could have caused the seismic sea wave and the distribution of damage reported in the sources”. Interestingly, the 1202 AD earthquake, which ruptured the Yammouneh fault (Daëron et al. 2004a, 2007) and produced a tsunami along the Lebanese coast and Cyprus (Guidoboni and Comastri 2005; Ambraseys 2009), exemplifies such a scenario, and it is no exception (Salamon et al. 2007).

The inland hypothesis, as favored above by Ambraseys (2009), can be demonstrated by three generic scenarios in line with Lebanese geology and seismotectonics. The first is the Lebanon Flexure, which runs along and west of the Yammaouneh Fault and builds the backbone of Mount Lebanon, represented by the Qartaba East Vergent Thrust Fault (after Daëron 2005; and Fig. 4–2 in Elias 2006). The second is a transverse fault, such as the Dahr el Baidar E–W-striking normal faults (Hancock and Atiya 1979), to which Salamon et al. (2003) attributed the June 3rd, 1983, Ml 4.9 earthquake. The third is one of the ENE–WSW strike-slip faults along the backbone of Mount Lebanon, west of the Yammouneh Fault, such as the Kelb-Bikfaya (Fig. 2–43 in Elias 2006; or Fig. 4–1 in Adonis) or Afka (Fig. 4–1 in Elias 2006) Faults.

Overall, and in line with the background described above, the simulated scenarios are generic representations of the proposed sources. Table 5 presents the fault rupture parameters we assigned to these sources to simulate the coseismic deformation they are able to induce. The results are presented on maps and discussed in Sect. 4.1.2.

**MLT and TBJD** represent offshore Lebanon sources characterized by parameters that have already been suggested in the published literature (Elias 2006, and Elias et al. 2007; and Faysal et al. 2023). This source strikes more or less parallel to the coast, with a shallow depth, relatively high dip, thrust or transpression mechanism, and considerable magnitude.

**Roum Fault:** We followed Nemer and Meghraoui (2006a, b), who identified 35 km long and shallow, mainly left-lateral strike-slip, fault and estimated an Ms of 7.1 for the 1837

**Table 5** Fault rupture parameters of potential 551 seismic sources

Source	A E N	B E N	Length (km)	Depth (km)	Width (km)	Strike (°)	Dip (°) / direction	Rake (°) / Mechanism	Offset (m)	Mag Mw	Source of information			
MLT/TBJD	35.29	33.71	35.76	34.53	100	20	30	25	45 / ESE	90	Thrust	2	7.4–7.6	Elias et al. (2007) / Faysal et al. (2023)
Roum Fault	35.57	33.20	35.57	33.62	50	20	20	360	90	0	Left L. SS	2–3	7.1–7.3	Darawcheh et al. (2000), Nemer and Meghraoui (2006a, b)
Lebanon Flexure	35.62	33.65	36.00	34.47	100–150	15	16	020	75 / ESE	90	Thrust	1–2	7.1–7.3	This work
Dahr el Baïdar	35.87	33.90	35.58	33.90	25	15	17	270	60 / N	–90	normal	1	6.7	Salamon et al. (2003)
Kelb-Bikfaya	35.60	33.90	35.92	34.00	30	15	15	NEN	90	180	Right l. SS	1	6.7	Elias (2006, Fig. 2–43)

Comments:

MLT: Offshore Mount Lebanon Thrust; TBJD: Tripoli-Batroun-Jounieh-Damour intermittent transpressive fault zone offshore Lebanon

Coordinates by decimal convention

All values are rounded

The strike directions are rounded, indicating that the dip direction is 90° clockwise of the strike direction

historical event. This source also represents Ambraseys's (2009) opinion that 551 was possibly on land on the Roum fault. In addition, Darawcheh et al. (2000, Figs. 1, 2 in there) located the source on land along a 50 km long trace of the strike-slip Roum fault, even though they mapped the 551 epicenter offshore of Beirut.

**Lebanon flexure:** This source is part of the structural system that thrusts the Lebanon mega-anticline (Fig. 4–2 in Elias 2006). It is a generic analog of the on-land MLT and TBJD and has similar mechanical characteristics.

**Dahr el Baidar** represents the seismotectonic potential of the E–W-striking normal fault system on-land Lebanon (Hancock and Atiya 1979), as has already been demonstrated by modern activity (Salamon et al. 2003). Its parameters were generalized accordingly to reflect the full rupture of such faults.

The **Kelb-Bikfaya** scenario exhibits yet another structural system that takes part in the deformation process associated with the restraining bend of the DST (see Fig. 2–43 in Elias 2006). This reference was used to characterize the source parameters of the maximal magnitude event.

We omitted the **Latakia Ridge** transpressive scenario (Nemer et al. 2023) for the reasons explained above. The computed coseismic deformation of the MLT and TBJD scenarios (discussed in Sect. 4.1.2) supports the view that the Latakia Ridge contribute negligible uplift of the marine-cut terraces along the Lebanese coast.

The **Bet-Zayda, Jordan Gorge Fault** (proposed by Wechsler et al. 2014), is a segment of the DST and is ~100 km south of Beirut and even south of the Roum Fault. Thus, as a strike-slip mechanism, the Bet-Zayda fault is expected to induce an insignificant coseismic effect along the Lebanese coast.

### 3.5 Potential tsunamigenic sources

The ongoing discussion on candidate earthquake and tsunami sources (Sect. 1.4) has resulted in an offshore earthquake that generated a tsunami (e.g., Elias et al. 2007) directly or via submarine landslide or an inland earthquake that triggered tsunamigenic submarine landslide (Ambraseys 2009). A third hypothesis is that an inland source near the coast triggered a tsunami through coseismic deformation extending offshore. To address this trilemma, we first searched for the seismogenic source (or sources) that best explained the macroseismic and environmental effects associated with the 551 event. Then, we used these sources to simulate the tsunami, and the scenario that best conforms to the reported tsunami effects was selected.

An interesting approach, previously presented by Salamon et al. (2007), suggests that a tsunami is generated by a chain of faults composed of the *Beirut Thrust Earthquake and the Roum fault*. The so-called *Beirut Thrust Earthquake* was proposed at the time by Darawcheh et al. (2000), Elias et al. (2001), and Daëron et al. (2004b) as the source of the 551 event, and the Roum Fault was suspected by Ambraseys (1997) to generate the 1837 AD earthquake. The tsunamigenic relevance of this source is discussed in Sect. 4.1.2 in light of the simulated Okada coseismic deformation.

The tsunamigenic potential of the Latakia Ridge (Faysal et al. 2023) is, in our view, limited because the “*Present plate kinematic vectors and earthquake data suggest that the movement along the eastern extent of the Cyprus Arc is largely sinistral strike-slip*” (Hall et al. 2005). Furthermore, the Bet-Zayda, Jordan Gorge Fault, a segment of the DST, is located too far away (~100 km) south of Beirut to induce considerable coseismic deformation. We thus skipped simulating tsunami generation from the abovementioned two

sources. Another potential source is the subaerial landslide in Lithoprosopon (Ras al-Shaqq) along the Botrys coast. Nonetheless, the limited volume of fresh mobilized submarine sediments offshore Ras-Chakka (Elias et al. 2007) questions the generation of considerable tsunamis by this source.

### 3.6 Bathymetry and topography grid

The grid used in our simulation was based on the bathymetry of the eastern Mediterranean Basin (30 m) from the EMODNET database (<https://tiles.emodnet-bathymetry.eu/>), and the topography of Lebanon was retrieved from the SRTM database (<https://www.earthdata.nasa.gov/sensors/srtm>). The two grids were then merged to build a digital elevation model. To better understand how Beirut, Berytus at the time, and its harbor were affected by the tsunami, we followed Marriner et al. (2008, Fig. 11), who proposed the location of the Beirut paleo-coastline at the time (blue line in Fig. 5, upper panel), and modified the simulation grid accordingly.

## 4 Modeling and simulations

### 4.1 Earthquake scenarios

#### 4.1.1 Iso-seismal map

Isoseismal maps portray lines of equally affected seismic intensities. In the case of historical earthquakes, when the source parameters are not known, resolving isoseismal maps and tracing the I<sub>max</sub> zone (the zone with the highest intensity degree) are important proxies for appraising the size and epicenter of a given event. Here, we converted the intensity degrees assigned to the 24 reported macroseismic effects, 25 environmental effects and 6 tsunami effects (Tables 2, 3, 4, respectively) into an inventory of 55 spatial data points in GIS format. This database (Supplementary Information 1 and the web map) allowed us to construct isoseismal maps and identify the I<sub>max</sub> zone of the 551 earthquake. Unfortunately, the historical accounts describe the end results of the two successive earthquakes without specifying what had happened in each of them; thus, we regard them as resulting from a single event. Consequently, we note that the amalgamation of the two events may have resulted in a greater magnitude and larger affected area, had we run the analysis on each event individually.

The statistics of the distribution of the data points were then tested to detect potential trends and verify their normality. The distribution of the intensities was close to normal, with a slight skewness to the right. Additionally, no north–south or east–west trends were detected, indicating that stochastic assumption can be applied. Thus, we implemented an Ordinary Kriging prediction to construct the isoseismal map and locate the potential I<sub>max</sub> region (e.g., de Rubeis et al. 2005; Teves-Costa et al. 2019). Two isoseismal maps were generated (Fig. 2). The first follows the conventional approach, which is based on macroseismic and EMS-98 intensities only (Fig. 2a), while the second (Fig. 2b) pursues a comprehensive perspective and integrates the three different scales (macroseismic, environmental and tsunami effects) onto a single map. For both maps, we applied 12 lags (that is, the bins in which pairs of data points are being compared and inspected) in which the minimum and maximum participating neighboring

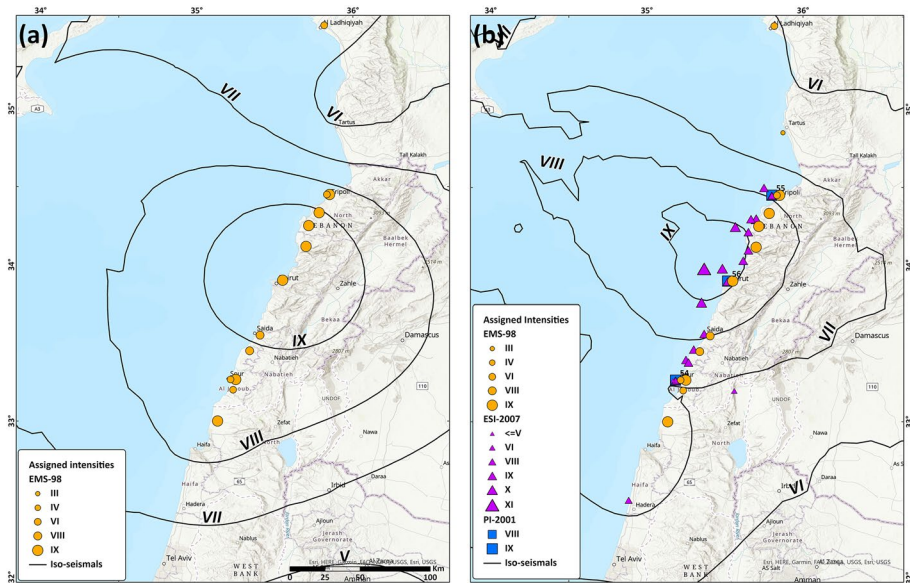


**Fig. 2** Proposed isoseismal maps of the 551 AD earthquake constructed by Ordinal Kriging prediction. In the left panel, **a** isoseismals interpolated on the basis of macroseismic data only; in the right panel, **b** isoseismals interpolated on the basis of all data points of macroseismic, environmental and tsunami effects. The legend presents only evaluated values, e.g., no degree V was assigned to any of the intensity scales; thus, intensity V is not present in the legend. The high degree isoseismals of the macroseismic data alone (map a) show a symmetrical pattern around the coast, preventing us from determining whether Imax (the suggested 551 source) is inland or offshore. The map of the combined data (map b) points, however, drags the Imax zone toward an offshore source, largely due to the presence of bathymetry surface rupture.

data points for prediction were set to 2 and 10, respectively. In the case of two overlapping points at the same geographic location (e.g., points representing EMS-98 and ESI-2007 values), the process averages the values of the two points and uses a single point instead to avoid overweighing.

The first map (Fig. 2a) shows that the concentration of data points along the Lebanese coast and the absence of information from inland or offshore drags the Imax zone toward the coast. However, the prediction containing all the data points (Fig. 2b) shifts the Imax zone slightly westward, suggesting a potential offshore source, largely due to the submarine surface rupture effects presented by Elias et al. (2007). Had additional inland or offshore points been available, the Imax zone might have been determined more decisively. Altogether, the map of the combined isoseismals (Fig. 2b) supports the notion that the 551 earthquake and tsunami source were triggered offshore, although its exact location cannot be determined.

#### 4.1.2 Okada coseismic deformation

We simulated the coseismic deformation resulting from the potential seismogenic sources of the 551 earthquake (Sect. 3.4 and Table 5). The modeled coseismic deformations were first examined to determine whether any of them closely reproduce the observed uplift of the marine-cut terraces along the Lebanese littoral zone (Sanlaville et al. 1997

and Morhange et al. 2006) and then used to simulate tsunami generation and propagation (Sect. 4.2).

Figure 3 presents the modeled coseismic deformations caused by the fault ruptures in the candidate scenarios (Table 5). Uplifted zones are represented by green and red tones, whereas subsided areas are represented by blue. The results clearly show that only the MLT-TBJD scenario (Fig. 3a) fully conforms to the uplifted marine-cut terraces (Fig. 3, thick black line along the coast north of Beirut). The Lebanon Flexure (Fig. 3b) produces subsidence of the terraces, and the other three sources, the Kelb-Bikfaya, Rour and Dahr el Baidar sources (Fig. 3c, d, e, respectively), affect the coastal region with slight conjugate

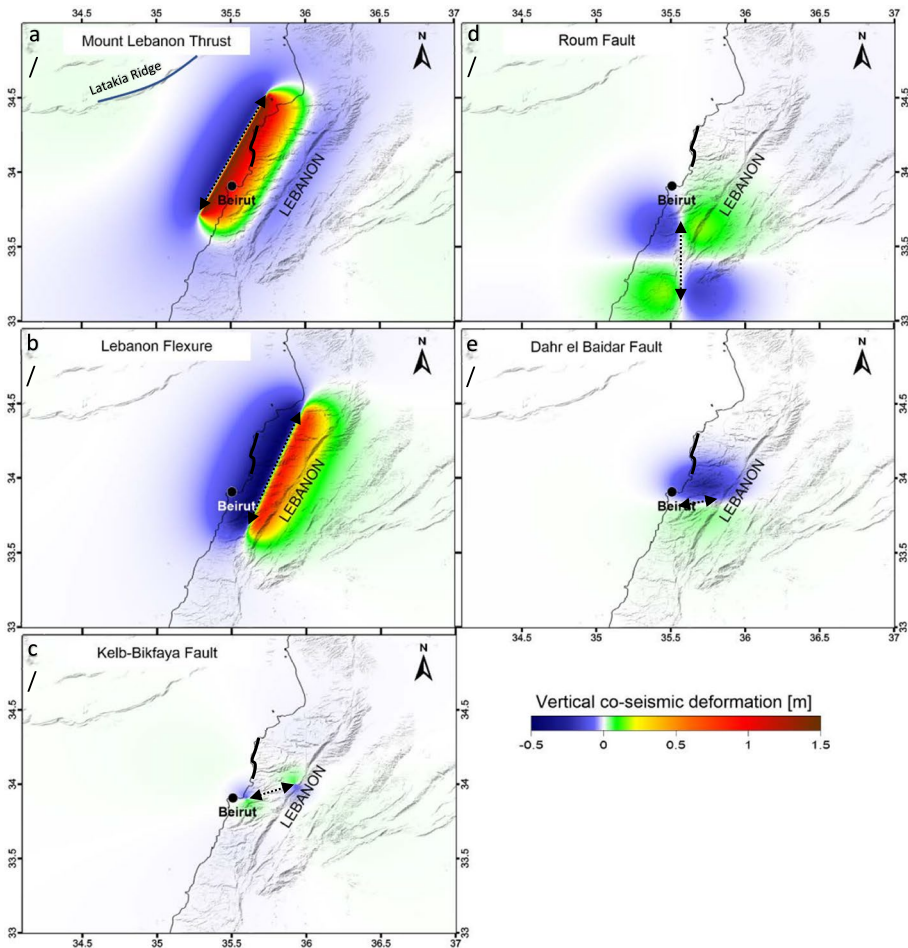


**Fig. 3** Modeled coseismic deformation generated by the potential 551 earthquake scenarios (Table 5). **a**: Mount Lebanon Thrust (MLT)—Tripoli-Batroun-Jounieh-Damour (TBJD); **b**: Lebanon Flexure; **c**: Kelb-Bikfaia Fault; **d**: Rour Fault; **e**: Dahr el Baidar Fault. Note the color-coded scale, where hot tones reflect uplift and cold tones indicate subsidence. The dashed, double-sided black arrow lines show the traces of the seismogenic fault. The thick black line along the coast, north of Beirut, denotes uplifted marine-cut terraces (modified from Elias et al. 2007)

uplift and subsidence. Thus, from the coseismic deformation results, the MLT-TBJD is considered the most plausible candidate seismogenic source for the 551 event.

Considering the potential coseismic effect of a strong earthquake along the Latakia Ridge and following Hall et al. (2005), who suggested that this fault is largely a left-lateral strike-slip source, the expected vertical effect is negligible. Furthermore, seismic profiles across the Latakia Ridge (in Hall et al. 2005) show that its northwestern side is expected to be uplifted, whereas the southeastern side that faces Beirut is expected to subside. This is opposed to the observed uplift of the marine-cut terraces along the Lebanese coast (Sanlaville et al. 1997; Morhange et al. 2006). Furthermore, if the southeastern side of the Latakia Ridge is uplifted by an earthquake equivalent to that in the MLT scenario, the associated coseismic effect should have faded out within ~50 km of the ridge, hardly affecting the Lebanese coast. According to Salamon et al. (2007), the *Beirut Thrust Earthquake*

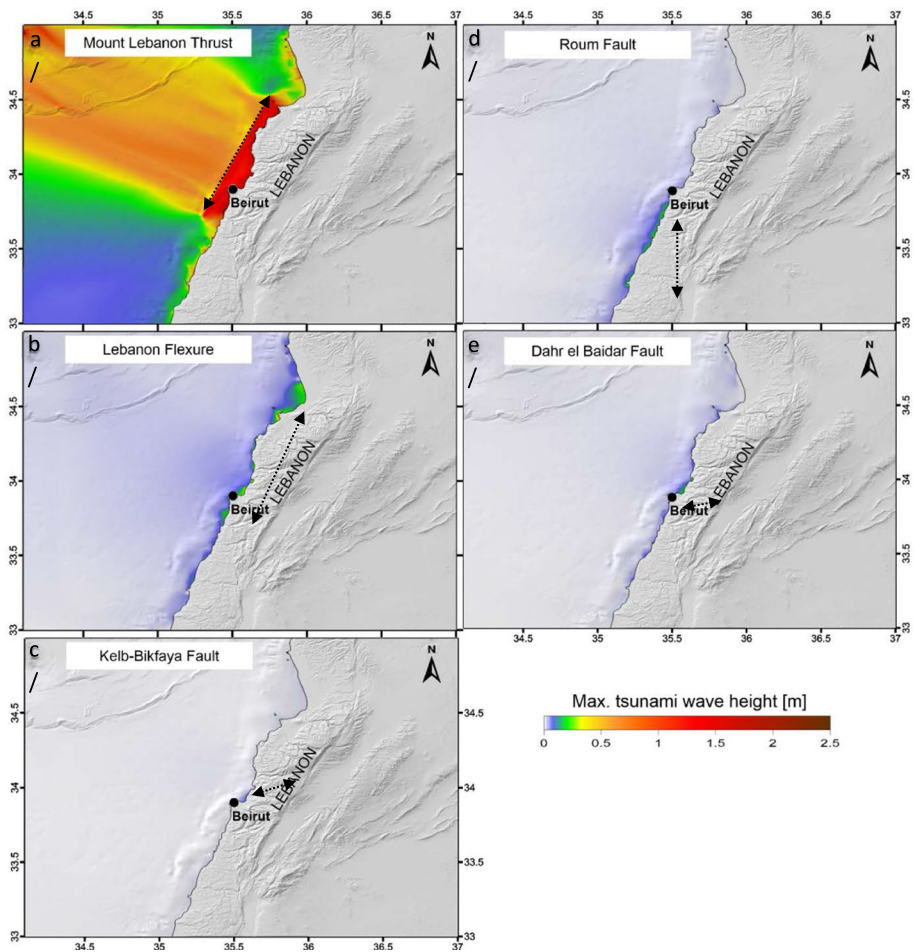


**Fig. 4** Modeled maximal tsunami wave heights generated by the potential 551 earthquake scenarios (Table 5). **a:** Mount Lebanon Thrust (MLT)—Tripoli-Batroun-Jounieh-Damour (TBJD); **b:** Lebanon Flexure; **c:** Kelb-Bikfaia Fault; **d:** Roum Fault; **e:** Dahr el Baidar Fault. Note the color-coded scale for tsunami wave heights. The dashed, double-sided arrow lines show the patterns of the seismogenic faults

scenario, which resembles the Roum Fault scenario (Fig. 3b), should have uplifted the marine-cut terraces north of Beirut and subsided the terraces south of Beirut. Morhange et al. (2006) showed that the terraces south of Beirut have been elevated.

## 4.2 Tsunami scenarios

The isoseismal interpolation (Fig. 2) and the simulation of the Okada coseismic deformation (Fig. 3) support the use of the MLT-TBJD as the optimal source of the 551 earthquake. Therefore, it became the preferred candidate for the 551 tsunamigenic origin, unless a significant seismogenic submarine landslide was also involved—of which we found no support (Sect. 3.5).

Here, we simulated tsunami generation and propagation by an MLT-TBJD source and examined whether the results agreed with previously reported observations. Our modeling of tsunami propagation was based on the nonlinear shallow water wave approximation, NSWING (Miranda et al. 2014). Additionally, we simulated tsunami wave propagation from the other proposed earthquake sources (Table 5 and Fig. 3) to understand the extent to which they agree with or differ from the MLT-TBJD source.

The results (Fig. 4) unequivocally show that MLT-TBJD is capable of producing a significant tsunami (Fig. 4a), which is far stronger than the other potential sources (Fig. 4b–e). While the MLT-TBJD source lifts 3 m waves all along the Lebanese coast (Fig. 4a), the others (Fig. 4b: Lebanon Flexure; 4c: Kelb-Bikfaia Fault; 4d: Roum Fault; and 4e: Dahr el Baidar Fault) reach hardly half a meter locally and along a limited stretch of the coast.

### 4.2.1 Synthetic tsunami time series generated by the MLT-TBJD source

The dramatic tragedy of the 551 disaster that is summarized by Ambraseys (2009) intrigued us to examine the time series of the tsunami waves that struck the Beirut coast:

*It is said that 30 000 (sic.) people were drowned by the sea wave, since, once the sea had retreated, they had gone down to the sea bed to plunder sunken wrecks [...]. Along the coast of Phoenice the sea receded for many hours by one to two miles (sic.), stranding sailing boats in the shallows. Then the sea came back, throwing ships on land, causing great havoc before returning to its original level.*

Despite the relatively informative description, quantitative details allowing comparison with numerical simulations are lacking. Specifically, there is no mention of arrival times, wave heights and phases, or extent of inundation. Most one can expect that simplification of the modeled scenario may, or may not, conform to the historical report.

We thus posted four artificial tide gauges off-coast Beirut (Table 6 and Fig. 5) and simulated synthetic waveforms generated by the MLT-TBJD tsunamigenic earthquake, which was found to be the preferred 551 source. All the synthetic mareograms (Fig. 5) show instantaneous coseismic uplift as high as 80 cm, followed by an immediate wave rise of several tens of cm and then a rapid and sharp decrease of approximately 3 m. The subsequent waves are mainly lower than the newly acquired height of the coast (due to ~80 cm of coseismic uplift). Generalizing the detailed simulation (Fig. 5, lower panels), we see immediate uplift of the coast followed by minor incoming waves, significant receding of the sea for approximately half an hour, and finally a gradual return to the original sea level. Thus, in our opinion, the general pattern of the simulated waves aligns with the historical description that emphasizes the retreat of the sea rather than the inundation inland.

**Table 6** Virtual tide gauge locations

Tide gauge	Coordinates Lat/Long
TG#1	33.9057 35.4938
TG#2	33.9055 35.5180
TG#3	33.9059 35.5503
TG#4	33.9083 35.5715
Beirut	33°54' 35°30'

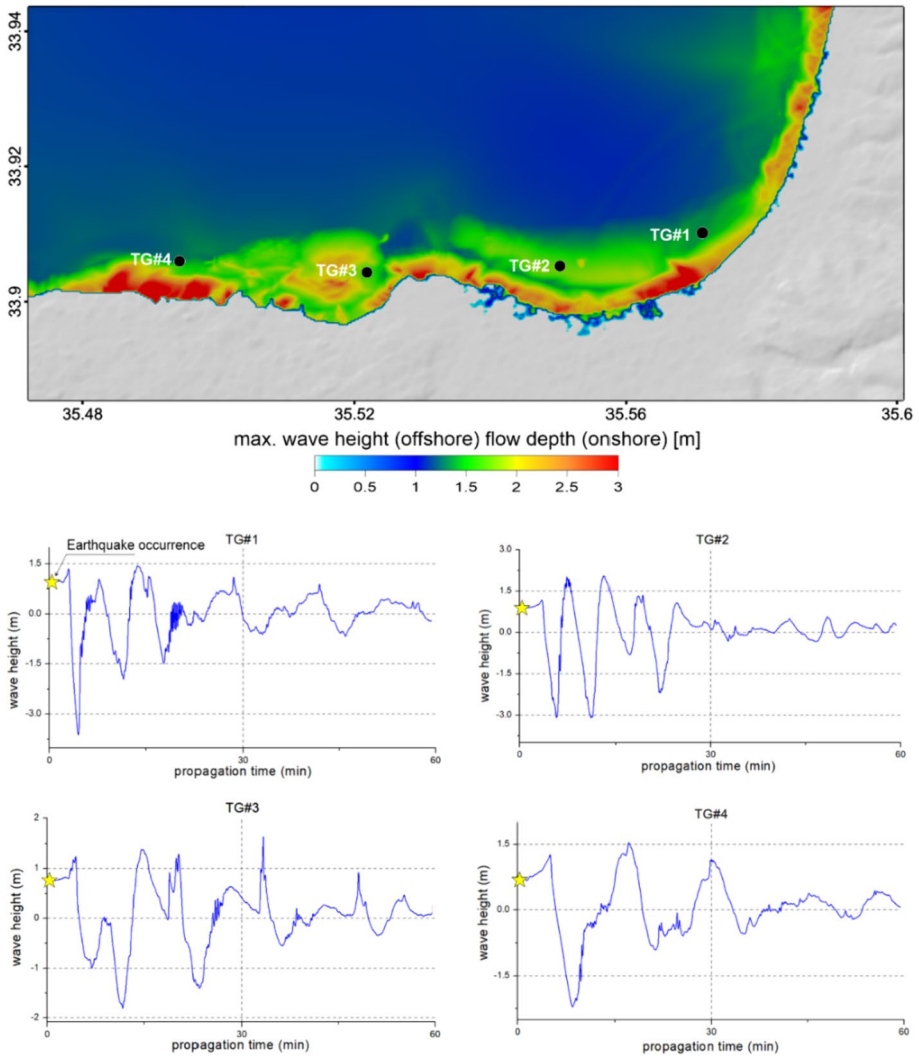


**Fig. 5** Upper panel: Map of the simulated maximal tsunami wave height and flow depth generated by the MLT-TBJD tsunamigenic source (Fig. 4a) in front of the Beirut coast. The locations of virtual tide gauges TG#1-4 are marked by black dots. Their shorter distances to the coastline, which is marked by the blue line, are 360 m for TG#1, 760 m for TG#2, 785 m for TG#3 and 505 m for TG#4. Lower panels: Synthetic tsunami time series generated by the MLT-TBJD source as recorded by the four artificial tide gauges (Table 6)

## 5 Discussion-between modeling and historical accounts

While historical accounts tend to be descriptive, qualitative, and subjective, modern investigations employ systematic methodology, standardized terminology, and quantitative analysis. Consequently, significant discrepancies exist between these two approaches, making it challenging to validate whether the modeling results are truly in line with the historical descriptions.

Our evaluation of the 551 event suggests that the modeled scenarios generally correspond to the historical accounts. However, a meticulous examination of the historical sources uncovers several inconsistencies that require careful analysis and explanation. In this context, we attempt to assess the apparent disparities perceived through a modern lens.

### 5.1 Limitations and uncertainties in data assessments and modelling

Although this work is the first quantitative assessment of the 551 earthquake and tsunami source, it still has limitations associated with uncertainties in the data and models used. These mainly concern historical data, their interpretation, and the modeling input and numerical codes. Historical reports commonly provide descriptions of past events that lack instrumental records. These data, while relevant, are mostly qualitative and vague, allowing multiple interpretations. To at least partially overcome this limitation, we applied rigorous selection criteria to the included studies. This approach mainly led to the exclusion of some repetitive reports and only relied on those that presented some coherence in describing the event and its consequences.

Models are another source of uncertainty in this study. The digital elevation model suffers from a lack of high-resolution coastal bathymetry, which can affect the reliability of the simulated nearshore tsunami propagation and coastal impact. However, mapping coastal bathymetric data is a high-cost and time-consuming task that we consider unnecessary, given the goal of this work. Another model limitation concerns the use of rectangular geometry and uniform slip distribution to represent earthquake fault ruptures, which overlooks their recognized complexity. Nevertheless, in the absence of seismic records for historical events, such simplified models remain valid for fairly representing seismic ruptures.

Tsunami generation and propagation models also have limitations. The first assumes that an instantaneous earthquake rupture allows the transfer of coseismic deformation to the sea surface. The second uses the shallow water approximation, assuming that the wavelength is larger than the water depth and that the vertical velocity component is constant in the water column, and neglecting wave dispersion while propagating away from the source area. However, despite the given limitations and uncertainties, the goal of this paper is not compromised, as the different earthquake scenarios produce very different radiation patterns.

### 5.2 Two shocks

The dramatic description of John of Ephesus: “*As the sea was rising up against them from behind, the earthquake brought down the city in front of them*” (translation by Guidoboni et al. 1994, and references in there) raises important questions. Translation of the same account by Ambraseys (2009): “*But when the sea rose up on those who were following them, an earthquake shattered the town before them*”, gives the same essence.

This means that the retreat of the sea occurred following the first shock, which exposed items on the seabed and attracted people to gather them. The retreat could have resulted from an ~M7 tsunamigenic earthquake or larger, strong enough to considerably drop the sea level, or a submarine landslide tsunami driven by an ~M6 earthquake or stronger (Salamon and Di Manna 2019).

The second shock occurred as the sea had already started to return, and it was strong enough to cause damage, possibly an earthquake of magnitude > 5.5 to 6 or even stronger. Was the first earthquake a main shock and the second one its aftershock, or the first event a preshock and the second one the main shock, or a strong doublet? Was the second event also tsunamigenic? Unfortunately, these questions remain open.

### 5.3 Movement of the sea

#### 5.3.1 "...the sea retreated for two miles"

Ambraseys (2009) summarized the historical reports, saying that "*Along the coast of Phoenice the sea receded for many hours by one to two miles ... stranding sailing boats in the shallows*". This is a considerable receding distance if taken by the face value of modern times, as well as a dramatic fall in sea level for stranding sailing boats on the sea floor. Extreme earthquake source parameters are needed to model such a dramatic scenario in which a significant retreat of the sea should be achieved along a wide and gently sloping continental shelf. However, the Beirut shelf is approximately 2 km wide and several tens of meters deep.

Therefore, it is also reasonable to assume that the '*two miles*' retreat distance is just a rough, subjective estimate given by eyewitnesses rather than an actual measurement and that it expresses the impression of the considerable distance the sea retreated. Such exaggerated quotes in historical reports are no exception. For example, Ambraseys (2009) quotes Michael the Syrian in regards to the January 18th, 746 or 749 earthquake in Palestine: "*Near Mt Tabor, a village moved four miles, with its houses and [other] buildings, without any stone's or a piece of adobe's falling from the buildings; and not a single man died, nor any animal, not even a chicken.*"

#### 5.3.2 "...the sea [...] returned to its original level"

According to Ambraseys (2009), the reported inundation was significant enough to throw ships on land, but there are no details on the range of inundation, especially with respect to the reported '*two miles*' retreat of the sea. Thus, it is reasonable to assume that the harbor area was inundated strongly enough to throw ships on land, but inland flooding may not have attracted special attention. Had the city of Beirut inundated, it might not have gone unnoticed by the historical account. This is also exhibited by our scenario modeling (Fig. 5).

Furthermore, there are no reports on a series of inbound and outbound motions of water, as is expected for significant tsunami events. Only the cause of great havoc before the sea returned to its original level is described. Here, again, the historical accounts may have generalized the chaos by telling us of the main phases: significant retreat of the sea, great havoc while returning, and returning to its normal position. In this sense, there is no mention of the first positive, low-amplitude arrival wave and the later wave series, as shown

by the modeling (Fig. 5). Geoarchaeological findings of scouring in Beirut harbor bedrock (Curvers and Stuart 2004), however, reveal considerable tsunami effects.

#### 5.4 Was Beirut the city most severely affected?

Most of the detailed descriptions relate to Beirut city and its marine environment. It seems that the Beirut harbor and offshore area were the most badly affected by the earthquake and the tsunami, with many casualties. Seemingly, geoarchaeological findings (Marriner et al. 2008) support this impression (see Sect. 1.3 above). Furthermore, the ensuing fire increased the damage and made it impossible to distinguish the relative impact caused by the two earthquakes, the tsunami and the fire.

At that time, Beirut was a central hub and administrative and industrial center (Mordechai 2019), and the earthquakes and the tsunami affected important structures. As a result, the disaster attracted much attention, and the descriptions were detailed. Reports on damage to other affected cities and harbors, however, are limited and are provided in general terms only. However, this does not necessarily mean that neighboring cities and rural settlements have suffered less than Beirut.

#### 5.5 Casualties and damage due to the tsunami

The historical accounts summarize the damage and casualties without detailing where, when and whether by earthquakes, tsunami or fire. At most, there is a mention of those drowned by the fast-returning wave in Beirut. In Ambraseys's (2009) opinion, the stated number of 30,000 casualties is grossly exaggerated.

No damage on land is attributed to the tsunami by the historical sources, only that the returning sea threw ships on land and caused great havoc before the sea returned to its original level (Ambraseys 2009). Geoarchaeological findings suggest intense scouring in the harbor seabed and that the damage in Beirut was mainly due to the earthquake and the ensuing fire.

#### 5.6 Alternative tsunamigenic sources

There seem to be contradictory interpretations regarding the volume of submarine mobilized sediments offshore Lebanon and hence its tsunamigenic potential. On the one hand, Elias (2006, Figs. 2–9, and p. 118) suggested that “*Nile derived turbidites were identified as the source of most of the Plio-Quaternary deposits in the southern and central Levantine basin [...]. In contrast, the thickness variation offshore Lebanon suggests a local onshore origin [...] Slump scars are frequent, especially along the outer shelf edge and slope, a telltale feature of transport by mass movement.*” On the other hand, Elias et al. (2007) suggest: “*The SHALIMAR data showed no evidence of submarine landslides except for small-scale slump scars and rockslides on or at the base of steep slopes south of Damour and near Batroun. It is thus possible to rule out the occurrence of a large local submarine landslide as a potential source of historical tsunamis along the Lebanese coast.*”

Faysal et al. (2023) hypothesize that the “... tsunamis could be generated by slope instabilities triggered by earthquakes along the Dead Sea Transform Fault”. Nonetheless, in their 3D bathymetry analysis, they do not single out any slope instability episode.

These observations raise the question whether the 551 tsunami was a triple sourced-mechanism of an earthquake, a submarine landslide and a subaerial landslide. Our findings are able to explain the historical descriptions of earthquakes and tsunamis with no need for secondary or tertiary sources, albeit some minor contributions from submarine and/or subaerial landslide tsunamis are still possible.

## 5.7 How coseismic uplift affects inundation

The simulated time series off-coast Beirut (Fig. 5) shows immediate coseismic uplift superimposed by a slight, first motion positive wave. Coming next is a series of waves in which the amplitudes of the negative phases are much larger than the amplitudes of the positive phases with respect to the just uplifted coast, after which the waves fade away. Overall, the simulation agrees with historical descriptions that emphasize the considerable receding of the sea for many hours (Sect. 5.3). The coseismic uplift of the Lebanese littoral zone, as evidenced by the uplifted marine-cut terraces (Sanlaville et al. 1997, and Morhange et al. 2006), seems to have counterbalanced the amplitude of the first tsunami wave that hit the coast. It is thus reasonable to assume that our simulated time series (Fig. 5) accords with the historical description.

Had the Beirut coast experienced coseismic subsidence, the amplitude of the positive waves would have been larger than the amplitude of the negative waves, which means greater inundation and less receding of the sea.

The 551 tsunamigenic earthquake exemplified the role of coseismic deformation in tsunami inundation when the seismogenic source was close to the coast. Coseismic uplift along the coast is expected to decrease inundation, whereas subsidence often increases tsunami flooding. This notion is important for tsunami hazard evaluation, as was already demonstrated by Salamon et al. (2021) for the Head of the Elat-Aqaba Gulf, by Gibbons et al. (2022) in Eastern Sicily, by Omira et al. (2016) along the Chilean coast and, in general, by Volpe et al. (2019).

## 6 Summary and key findings

Here, we reassessed the historical accounts and modern discoveries associated with the July 9, 551 AD earthquakes and tsunami that affected the Phoenician (Lebanon) coast. Our unique contribution focused on resolving the potential sources of these events by modeling their expected coseismic deformation and resulting tsunami and verifying whether the computed scenarios conform to the authentic reports and findings.

First, we reviewed the available information and collected reports of macroseismic, environmental and tsunami effects that were screened carefully, found to be reliable and published in peer-reviewed literature. We then standardized and merged these disparate sources into a coherent database (Tables 2, 3, 4) and assigned intensity degrees to each of the given effects (Fig. 1b). Such integration and homogenization are justified since the intensity degrees of the three modern scales of macroseismic (EMS-98), environmental (ESI-2007) and tsunami (PI-2001) effects correspond to each other.

The integrated intensity database was then used to construct an isoseismal map (Fig. 2b) that points the area of highest shaking intensities ( $I_{max}$ ) toward offshore Lebanon, primarily due to the likely presence of fresh bathymetry scarps. While these scarps were interpreted by Elias et al. (2007) as sea-bottom ruptures induced by the 551 seismogenic

source, Faysal et al. (2023) related them to surface disturbances due to salt tectonics. We thus assigned these environmental effects low reliability only (Table 4). Overall, however, it is reasonable to assume that the 551 tsunami source is also located within the zone with the highest intensity.

Next, we employed Okada's (1985) half-space elastic equations to model the coseismic deformation associated with various earthquake sources proposed in the literature for the 551 event (Table 5). It appears that the MLT-TBJD best accords with the evidence of uplifted marine-cut terraces along the Lebanese coast (Sanlaville et al. 1997; and Morhange et al. 2006). In the following step, we employed the nonlinear shallow water code NSWING (Miranda et al. 2014), which was successively used and benchmarked in other studies (Baptista et al. 2016, 2020; Omira et al. 2016) with a system of nested grids, for numerical modeling of the ensuing tsunami.

To better replicate the effect of the tsunami on Beirut, we reconstructed Beirut's paleo-coastline at that time (after Marriner et al. 2008, Fig. 11). However, again, among the tsunami-modeled sources, the MLT-TBJD better accords with the historical reports (Fig. 4a). The synthetic waveforms reaching offshore Beirut reveal the interaction between the coseismic deformation, wave heights and inundation (Fig. 5). Here, the seafloor at the artificial tide gauge locations is first uplifted (by coseismic deformation), and then the motion of the modeled sea surface elevation is recorded. The initial sea surface elevation is thus the coseismic uplift at the given tide-gauge site (yellow stars in Fig. 5, lower panels). As a result, the height of the ensuing waves is reduced along the nearby coast. Overall, the net effect of tsunami waves and inundation on a given coast is the result of coseismic deformation and the height of the attacking wave.

## 7 Understanding and conclusions

We have learned that engaging raw data, historical accounts, environmental evidence and geoarchaeological findings with careful modeling generates fruitful dialog and improves the understanding of both the original accounts and the seismo-tsunamigenic process. Overall, the modeled earthquake and tsunami source that best conforms to the 551 AD historical descriptions and macroseismic, environmental and tsunami effects are most likely an MLT-TBJD with a magnitude of  $\sim 7.5$ . Indeed, Faysal et al. (2023) challenged the existence of the MLT and instead proposed the remote, 70 km away, trans-pressure/tension Latakia Ridge. In our opinion, the localized zone of the transpressive TBJD fault system proposed by Faysal et al. (2023) is similar to the MLT of Elias et al. (2007) in producing coseismic uplift along the Lebanese coast and generating a tsunami. Thus, rather than a specific fault, our MLT-TBJD scenario should be regarded as a generic representation of a potential seismogenic and tsunamigenic source of the 551 event. Although some questions, such as resolving the two 551 AD shocks and the potential contributions of submarine and/or sub-aerial tsunamigenic landslides, are left open, central issues are better clarified.

Most important are the resolving of the MLT-TBJD as the 551 AD earthquake and tsunami source and the effect of the associated coseismic uplift along the coast on the incoming waves and shifting the impact of the tsunami on receding of the sea rather than severe inundation. In fact, the results show that there is no need to include a submarine landslide source to explain the overall observations of the 551 tsunami, even though a minor contribution of such a source cannot be excluded.

## 7.1 Avenues for future research

According to our 551 investigation, there are several information and knowledge gaps to close, yet they are not trivial at all. Following an ordered methodology and evaluating the existing information, we found that the evidences of bathymetry surface ruptures (Elias et al. 2007) are a ‘game changer’. It drew the Imax zone toward offshore Lebanon and suggested placing an earthquake source capable of generating a considerable tsunami and allowed us to explain all the available 551 catastrophe evidence. However, Faysal et al. (2023) related these ruptures to local salt tectonics. To be resolved, future investigations are still needed to determine whether these ruptures were driven solely by shallow salt tectonics or might have also been generated by deeper crustal deformation forces.

The above discussion exemplifies the need for a continuous search and research of data, evidence and understanding from all available disciplines, addressing not only the 551 event but also the associated dilemmas. In particular, exploring additional historical accounts, geological evidence and archaeoseismic findings related to the 551 event is expected to improve the reconstruction of its effects, resolving the share of damage among the two earthquakes, the tsunami and the ensuing fire, and retracing its seismo- and tsunamigenic sources.

On a broader scale, it is clear that strong shallow, near-offshore earthquakes can generate coseismic deformation as well as subaerial and submarine landslides, which in turn can induce multisource tsunamis. However, resolving the reverse, that is, separating a given tsunami into its generating components, is not simple and needs further investigation.

The impact of coseismic deformation on tsunami hazards was clearly demonstrated (Sect. 5.7). Thus, future site-specific tsunami hazard investigations should consider special care when the nearby coast experiences subsidence. This notion also necessitates realistic tsunami risk and damage evaluation, if such a configuration applies, either offshore Lebanon or along the Levantine coasts, and elsewhere in the world.

**Supplementary Information** The online version contains supplementary material available at <https://doi.org/10.1007/s11069-024-06559-4>.

**Acknowledgements** A.S. acknowledges Professor Ricardo M. Trigo, the Director of Instituto Dom Luiz, Faculdade de Ciências da Universidade de Lisboa (IDL-FCUL), Portugal, for inviting and spending his sabbatical leave there. Special thanks are due to Professor Miguel Miranda, President of the Board of Directors of the Portuguese Institute for Sea and Atmosphere (IPMA), for the homely welcome. IPMA and IDL-FCUL are highly appreciated for hosting AS during the COVID-19 pandemic. The detailed review and useful comments and suggestions provided by the two anonymous reviewers are highly acknowledged and appreciated. This work was partially funded by the Portuguese Fundação para a Ciência e a Tecnologia (FCT) I.P./MCTES through national funds (PIDDAC) – UIDB/50019/2020. Open access funding was provided by the Geological Survey of Israel.

**Author Contributions** Amos Salamon, Maria Ana Baptista and Rachid Omira conceptualized and planned the methodology and designed the project. Amos Salamon led the project, collected the data and prepared the main draft. Maria Ana Baptista supervised the re-evaluation of the historical data and hazard assessment and directed the discussion. Rachid Omira simulated the Okada coseismic deformation, tsunami scenarios and waveforms and prepared the relevant text and Figs. 3, 4 and 5. Moti Zohar prepared the location map in Fig. 1, performed the statistics of the database, produced the isoseismal maps in Fig. 2 and prepared the relevant text. All authors reviewed and commented on all forms of the manuscript and read and approved the final version.

**Funding** Open access funding provided by Geological Survey of Israel. This work was partially funded by the Portuguese Fundação para a Ciência e a Tecnologia (FCT) I.P./MCTES through national funds (PIDDAC) – UIDB/50019/2020.

**Data availability** All data collected, generated and analyzed during this study are included in this published article and credited in the list of references.

## Declarations

**Conflict of interest** The authors have no relevant financial or nonfinancial interests to disclose or competing interests to declare that are relevant to the content of this article.

**Open Access** This article is licensed under a Creative Commons Attribution 4.0 International License, which permits use, sharing, adaptation, distribution and reproduction in any medium or format, as long as you give appropriate credit to the original author(s) and the source, provide a link to the Creative Commons licence, and indicate if changes were made. The images or other third party material in this article are included in the article's Creative Commons licence, unless indicated otherwise in a credit line to the material. If material is not included in the article's Creative Commons licence and your intended use is not permitted by statutory regulation or exceeds the permitted use, you will need to obtain permission directly from the copyright holder. To view a copy of this licence, visit <http://creativecommons.org/licenses/by/4.0/>.

## References

- Ambraseys NN (1997) The earthquake of 1 January 1837 in Southern Lebanon and Northern Israel. *Ann Geofis* 40:923–935
- Ambraseys NN (2009) Earthquakes in the Mediterranean and Middle East: a multidisciplinary study of seismicity up to 1900. Cambridge University Press, Cambridge, p 968
- Baptista MA, Miranda JM, Batlló J, Lisboa F, Luis J, Maciá R (2016) New study on the 1941 Gloria Fault earthquake and tsunami. *Nat Hazards Earth Syst Sci* 16(8):1967–1977
- Baptista MA, Miranda JM, Omira R, El-Hussain I (2020) Study of the 24 September 2013 Oman Sea tsunami using linear shallow water inversion. *Arab J Geosci* 13(14):606
- Ben-Menahem A (1991) Four thousand years of seismicity along the Dead Sea rift. *J Geophys Res* 96(B12):195–216
- Beyth M, Sagy A, Hajazi H, Alkhraisha S, Mushkin A, Ginat H (2018) New evidence on the accurate displacement along the Arava/Araba segment of the Dead Sea Transform. *Int J Earth Sci* 107:1431–1443. <https://doi.org/10.1007/s00531-017-1549-7>
- Brax M, Albini P, Beauval C, Jomaa R, Sursock A (2019) An earthquake catalog for the Lebanese Region. *Seismol Res Lett* 90(6):2236–2249. <https://doi.org/10.1785/0220180292>
- Curvers H, Stuart B (2004) Beirut Central District Archaeology Project. 1994–2003. In: Doumet-Serhal C (Ed.) *Decade: A Decade of Archaeology and History in the Lebanon*. Archaeology and History of Lebanon, Beirut 248–260
- Daëron M (2005) *Rôle, cinématique et comportement sismique à long terme de la faille de Yammouneh*. Laboratoire de Sismotectonique. Paris, IGP
- Daëron M, Benedetti L, Tapponnier P, Sursock A, Finkel RC (2004a) Constraints on the post ~25-ka slip rate of the Yammouneh fault (Lebanon) using in situ cosmogenic <sup>36</sup>Cl dating of offset limestone-clast fans. *Earth Planet Sci Lett* 227:105–119. <https://doi.org/10.1016/j.epsl.2004.07.014>
- Daëron M, Elias A, Klinger Y, Tapponnier P, Jacques E, Sursock A (2004b) Sources of the AD 551, 1202 and 1759 earthquakes (Lebanon and Syria). American Geophysical Union, Fall Meeting 2004, abstract #T41F-1294
- Daëron M, Klinger Y, Tapponnier P, Elias A, Jacques E, Sursock A (2007) 12,000-year-long record of 10 to 13 Paleoequakes on the Yammouneh Fault, Levant Fault System. *Lebanon Bull Seismol Soc Am* 97(3):749–771. <https://doi.org/10.1785/0120060106>
- Darawcheh R, Margottini C, Paolini S (2000) The 9 July 551 Beirut Earthquake, Eastern Mediterranean region. *J Earthq Eng* 4:403–414
- Darawcheh R, Hasan A, Abdul-Wahed MK (2022) Seismotectonics of the easternmost Cypriot Arc: an active plate boundary. *J African Earth Sci* 187:104447. <https://doi.org/10.1016/j.jafrearsci.2021.104447>
- de Rubeis V, Tosi P, Gasparini G, Solipaca A (2005) Application of Kriging technique to seismic intensity data. *Bull Seismol Soc Am* 95(2):540–548

- Dey H, Goodman-Tchernov B, Sharvit J (2014) Archaeological evidence for the tsunami of January 18, 749 Islamic: a chapter in the history of Early Caesarea, Qaysariyah (Caesarea Maritima). *J Rom Archaeol* 27:357–373
- Dubertret L (1955) Carte géologique du Liban. République Libanaise, Ministère des Travaux Publics, Beirut
- Elias A (2006) Le Chevauchement de Tripoli-Saida: Croissance du Mont-Liban et risque sismique. Thèse de Doctorat en Géophysique Interne, IPG-Paris, Laboratoire de Tectonique, Mécanique de la Lithosphère (In English, French abstract)
- Elias AP, Tapponnier M, Daéron E, Jacques A Surssock, King G (2001) The Tripoli-Roum thrust: source of the Beirut 551 AD earthquake and cause of the rise of Mount-Lebanon (abstract). *EOS Trans. AGU* 82, no. 47 (Fall Meet. Suppl.), S12D-0636
- Elias A, Tapponnier P, Singh SC, King GCP, Briaris A, Dearon M, Carton H, Surssock A, Jaques E, Jomaa R, Klinger Y (2007) Active thrusting offshore Mount Lebanon: Source of the tsunamigenic A.D. 551 Beirut-Tripoli earthquake. *Geology* 35:755–758. <https://doi.org/10.1130/G23631A.1>. [DataRepositoryitem2007190](https://doi.org/10.1130/G23631A.1)
- Faysal R, Nemer T, Sarieddine K (2023) Investigating the geological fault framework offshore Lebanon: insight into the earthquake geology of the eastern mediterranean region. *Pure Appl Geophys* 180:3249–3268. <https://doi.org/10.1007/s00024-023-03336-5>
- Freund R, Garfunkel Z, Zak I, Goldberg M, Weissbrod T, Derin B, Bender F, Wellings FE, Girdler RW (1970) The shear along the Dead Sea rift [and discussion]. *Philos Trans R Soc Lond, Math Phys Sci* 267:107–130. <https://doi.org/10.1098/rsta.1970.0027>
- Garfunkel Z (1981) Internal structure of the Dead Sea leaky transform (rift) in relation to plate kinematics. *Tectonophysics* 80:81–108. [https://doi.org/10.1016/0040-1951\(81\)90143-8](https://doi.org/10.1016/0040-1951(81)90143-8)
- Garfunkel Z (2010) The long- and short-term lateral slip and seismicity along the Dead Sea Transform: an interim evaluation. *Israel J Earth Sci* 58:217–235
- Garfunkel Z (2014) Lateral motion and deformation along the Dead Sea transform. In: Garfunkel Z, Ben-Avraham Z, Kagan A (Eds) *Dead Sea Transform System Reviews*, Springer Science Business Media, Dordrecht, The Netherlands, 109–151
- Garfunkel Z, Almagor G (1985) Geology and structure of the continental margin off Northern Israel and the adjacent part of the Levantine Basin. *Mar Geol* 62:105–131
- Gibbons SJ, Lorito S, de la Asunción M, Volpe M, Selva J, Macías J, Sánchez-Linares C, Brizuela B, Vöge M, Tonini R, Lanucara P, Glimsdal S, Romano F, Meyer JC, Løvholt F (2022) The sensitivity of tsunamis impact to earthquake source parameters and manning friction in high-resolution inundation simulations. *Front Earth Sci* 9:757618. <https://doi.org/10.3389/feart.2021.757618>
- Gomez F, Meghraoui M, Darkal AN, Hijazi F, Mouty M, Suleiman Y, Sbeinati R, Darawcheh R, Al-Ghazzi R, Barazangi M (2003) Holocene faulting and earthquake recurrence along the Serghaya branch of the Dead Sea fault system in Syria and Lebanon. *Geophys J Int* 153:658–674
- Gomez F, Khawlie M, Tabet C, Darkal AN, Khair K, Barazangi M (2006) Late Cenozoic uplift along the northern Dead Sea transform in Lebanon and Syria. *Earth Planet Sci Lett* 241:913–931. <https://doi.org/10.1016/j.epsl.2005.10.029>
- Gomez F, Karam G, Khawlie M, McClusky S, Vernant P, Reilinger R, Jaafar R, Tabet C, Khair K, Barazangi M (2007) Global Positioning System measurements of strain accumulation and slip transfer through the restraining bend along the Dead Sea fault system in Lebanon. *Geophys J Int* 168:1021–1028. <https://doi.org/10.1111/j.1365-246X.2006.03328.x>
- Gomez F, Cochran WJ, Yassminh R, Jaafar R, Reilinger R, Floyd M, King RW, Barazangi M (2020) Fragmentation of the Sinai Plate indicated by spatial variation in present-day slip rate along the Dead Sea Fault System. *Geophys J Int* 221:1913–1940. <https://doi.org/10.1093/gji/ggaa095>
- Goodman-Tchernov BN, Austin JA Jr (2015) Deterioration of Israel's Caesarea Maritima's ancient harbor linked to repeated tsunami events identified in geophysical mapping of offshore stratigraphy. *J Archaeol Sci Rep* 3:444–454
- Goodman-Tchernov BN, Dey HW, Reinhardt EG, McCoy F, Mart Y (2009) Tsunami waves generated by the Santorini eruption reached Eastern Mediterranean shores. *Geology* 37:943–946. <https://doi.org/10.1130/G25704A.1>
- Grünthal G (Ed.) (1998) European Macroseismic Scale 1998, Cahiers du Centre Européen de Géodynamique et de Seismologie, 15, Conseil de l'Europe, Luxembourg, 99 pp
- Guidoboni E, Comastri A, Traina G (1994) Catalogue of ancient earthquakes in the Mediterranean area up to the 10th Century. ING-SGA, Rome-Bologna, Italy, p 504
- Guidoboni E, Comastri A (2005) Catalogue of Earthquakes and Tsunamis in the Mediterranean from the 11th to the 15th Century. Istituto Nazionale di Geofisica e Vulcanologia, Rome
- Guidoboni E, Ebel JE (2009) Earthquakes and tsunamis in the past: a guide to techniques in historical seismology. Cambridge University Press, New York

- Gvirtzman Z, Zilberman E, Folkman Y (2008) Reactivation of the Levant passive margin during the late Tertiary and formation of the Jaffa Basin offshore central Israel. *J Geol Soc* 165:563–578. <https://doi.org/10.1144/0016-76492006-200>
- Gwiazda M, Waliszewski T (2014) Early Byzantine residential architecture in Jiyeh (Porphyreon) after excavation season in 2012 and 2013. *Archeologia* 65(2014):35–56
- Hall J, Aksu AE, Calon TJ, Yaşar D, (2005) Varying tectonic control on basin development at an active microplate margin: Latakia Basin Eastern Mediterranean. *Mar Geol* 221(1–4):15–60. <https://doi.org/10.1016/j.margeo.2004.05.034>
- Hamiel Y, Piatibratova O (2021) Spatial variations of slip and creep rates along the southern and central Dead Sea Fault and the Carmel–Gilboa Fault System. *J Geophys Res Solid Earth* 126:e2020JB021585. <https://doi.org/10.1029/2020JB021585>
- Hancock PL, Atiya MS (1979) Tectonic significance of mesofracture systems associated with the Lebanese segment of the Dead Sea transform fault. *J Struct Geol* 1:143–153
- Huijser C, Harajli M, Sadek S (2016) Re-evaluation and updating of the seismic hazard of Lebanon. *J Seismol* 20:233–250. <https://doi.org/10.1007/s10950-015-9522-z>
- Kagan E, Stein M, Agnon A, Neumann F (2011) Intrabasin paleoearthquake and quiescence correlation of the late Holocene Dead Sea. *J Geophys Res* 116:B04311. <https://doi.org/10.1029/2010JB007452>
- Kanari M, Katz O, Weinberger R, Porat N, Marco S (2019) Evaluating earthquake-induced rockfall hazard near the Dead Sea Transform. *Nat Hazards Earth Syst Sci* 19:889–906. <https://doi.org/10.5194/nhess-19-889-2019>
- Karcz I (2004) Implications of some early Jewish sources for estimates of earthquake hazard in the Holy Land. *Ann Geophys* 47:759–792
- Katz O, Reuven E, Aharonov E (2015) Submarine landslides and fault scarps along the eastern Mediterranean Israeli continental-slope. *Mar Geol* 369:100–115. <https://doi.org/10.1016/j.margeo.2015.08.006>
- Krenkel, (1924) *Der Syrische Bogen*. *Zentralbl Mineral* 9:274–281
- Marco S (2008) Recognition of earthquake-related damage in archaeological sites: examples from the Dead Sea fault zone. *Tectonophysics* 453:148–156
- Marco S, Klinger Y (2014) Review of on-fault palaeoseismic studies along the dead sea fault. In: Garfunkel Z, Ben-Avraham Z, Kagan A (Ed) *Dead Sea Transform System Reviews*. Springer Science Business Media, Dordrecht, The Netherlands, Chapter 7, 183–205
- Marriner N, Morhange C, Saghih-Beydoun S (2008) Geoarchaeology of Beirut’s ancient harbour, Phoenicia. *J Archaeol Sci* 35:2495–2516
- Meghraoui M (2015) Paleoseismic history of the dead sea fault zone. In: Beer M, Kougioumtzoglou I, Patelli E, Au IK (eds) *Encyclopedia of Earthquake Engineering*. Springer, Berlin, Heidelberg. [https://doi.org/10.1007/978-3-642-36197-5\\_40-1](https://doi.org/10.1007/978-3-642-36197-5_40-1)
- Michetti AM, Esposito E, Gëurpinar A, Mohammadioun B, Mohammadioun J, Porfido S, Roghazin E, Serva L, Tatevossian R, Vittori E, Audemard F, Comerci V, Marco S, McCalpin J, Mörner NA (2004) The INQUA scale. An innovative approach for assessing earthquake intensities based on seismically-induced ground effects in natural environment. In: Vittori E, Comerci V (ed) *Memorie Descrittive della Carta Geologica d’Italia*, APAT, Roma, LXVII-116
- Migowski C, Agnon A, Bookman R, Negendank JFW, Stein M (2004) Recurrence pattern of Holocene earthquakes along the Dead Sea transform revealed by varve counting and radiocarbon dating of lacustrine sediments. *Earth Planet Sci Lett* 222(1):301–314
- Miranda JM, Luis JF, Reis C, Omira R, Baptista MA (2014) Validation of NSWING, a multi-core finite difference code for tsunamis propagation and run-up. American Geophysical Union (AGU) fall meeting, San Francisco. Paper (No. S21A-4390)
- Mordechai L (2019) Berytus and the aftermath of the 551 earthquake. *U Schyłku Starożytności: Studia Źródłoznawcze*, (17/18), 198–241. <https://doi.org/10.36389/UW.USS.18-19.1.7>
- Morhange C, Pirazzoli PA, Marriner N, Montaggioni LF, Nammour T (2006) Late Holocene relative sea-level changes in Lebanon, Eastern Mediterranean. *Mar Geol* 230:99–114
- Musson RM, Cécic I (2012) Intensity and Intensity Scales. In: Bormann P (Ed) *New Manual of Seismological Observatory Practice 2 (NMSOP-2)*. Potsdam : Deutsches GeoForschungsZentrum GFZ, 1–41. [https://doi.org/10.2312/GFZ.NMSOP-2\\_ch12](https://doi.org/10.2312/GFZ.NMSOP-2_ch12)
- Nemer T, Meghraoui M (2006) Evidence of coseismic ruptures along the Roum fault (Lebanon): a possible source for the AD 1837 earthquake. *J Struct Geol* 28:1483–1495
- Nemer T, Meghraoui M, Gomez F (2006) Active deformation and seismogenic potential of the main subsidiary faults within the Lebanese Restraining Bend along the Dead Sea Transform (Lebanon). AGU Fall Meeting. AGU Fall Meeting, San Francisco, California, 2006

- Nemer T, Meghraoui M, Khair K (2008) The Rachaya-Serghaya fault system (Lebanon). Evidence of Coseismic ruptures and the AD 1759 earthquake sequence. *J Geophys Res* 113:B05312. <https://doi.org/10.1029/2007JB005090>
- Nemer TS, Vaccari F, Meghraoui M (2023) Seismic hazard assessment of the lebanese restraining bend: a neo-deterministic approach. *Pure Appl Geophys* 180:1835–1859. <https://doi.org/10.1007/s00024-023-03233-x>
- Okada Y (1985) Surface deformation due to shear and tensile faults in a half-space. *Bull Seismol Soc Am* 75:1135–1154
- Omira R, Baptista MA, Lisboa F (2016) Tsunami Characteristics Along the Peru-Chile Trench Analysis of the 2015 Mw8.3 Illapel, the 2014 Mw8.2 Iquique and the 2010 Mw8.8 Maule Tsunamis in the Near-field. *Pure Appl Geophys* 173(4):1063–1077. <https://doi.org/10.1007/s00024-016-1277-0>
- Papadopoulos GA, Imamura F (2001) A proposal for a new tsunami intensity scale. *International Tsunami symposium 2001 Proc.*, Seattle, Washington, Aug. 7–10: 569–577
- Papadopoulos GA, Gr`acia E, Urgeles R, Sallares V, De Martini PM, Pantosti D, Gonz`alez M, Yalciner AC, Mascle J, Sakellariou D, Salamon A, Tinti S, Karastathis V, Fokaefs A, Camerlenghi A, Novikova T, Papageorgiou A, (2014) Historical and pre-historical tsunamis in the Mediterranean and its connected seas: Geological signatures, generation mechanisms and coastal impacts. *Mar Geol* 354:81–109. <https://doi.org/10.1016/j.margeo.2014.04.014>
- Porat N, Duller GAT, Amit R, Zilberman E, Enzel Y (2009) Recent faulting in the southern Arava, Dead Sea Transform: Evidence from single grain luminescence dating. *Quat Int* 199(1–2):34–44
- Quennell AM (1959) Tectonics of the Dead Sea rift. 20th Int Geol Cong (1956), Assoc Afr Geol Surv pp 385–405
- Salamon A (2011) Potential tsunamigenic sources in the eastern Mediterranean and a decision matrix for a tsunami early warning system. In: Briand F (ed) *Marine Geo-hazards in the Mediterranean*. CIESM Workshop Monograph n° 42, 42. CIESM Publisher, Monaco, pp. 35–42, 192 p
- Salamon A, Di Manna P (2019) Empirical constraints on magnitude distance relationships for seismically-induced submarine tsunamigenic landslides. *Earth-Sci Rev* 191:66–92. <https://doi.org/10.1016/j.earscirev.2019.02.001>
- Salamon A, Hofstetter A, Garfunkel Z, Ron H (2003) Seismotectonics of the Sinai subplate—the eastern Mediterranean region. *Geophys J Int* 155(1):149–173
- Salamon A, Rockwell T, Ward S, Guidoboni E, Comastri A (2007) Tsunami hazard evaluation of the eastern Mediterranean: Historical analysis and selected modelling. *Bull Seismol Soc Am* 97(3):705–724
- Salamon A, Rockwell T, Guidoboni E, Comastri A (2011) A critical evaluation of tsunami records reported for the Levant coast from the second millennium BCE to the present. *Israel J Earth Sci* 58:327–354
- Salamon A, Frucht E, Ward SN, Gal E, Grigorovitch M, Shem-Tov R, Calvo R, Ginat H (2021) Tsunami Hazard Evaluation for the Head of the Gulf of Elat-Aqaba. *Northeastern Red Sea Front Earth Sci* 8:602462. <https://doi.org/10.3389/feart.2020.602462>
- Sanlaville P (1977) *Etude géomorphologique de la région littorale du Liban* [Ph.D. thèse]: Beirut, Lebanese University, 859 p
- Sanlaville P, Dalongeville R, Bernier P, Evin J (1997) The Syrian coast: a model of Holocene coastal evolution. *J Coast Res* 13(2): 385–396
- Serva L, Vittori E, Comerci V, Esposito E, Guerrieri L, Michetti AM, Mohammadioun B, Mohammadioun GC, Porfido S, Tatevossian RE (2016) Earthquake hazard and the environmental seismic intensity (ESI) scale. *Pure Appl Geophys* 173(5):1479–1515
- Singh S (2003) SHALIMAR cruise, RV Le Suroît. <https://doi.org/10.17600/3020120>.
- Teves-Costa P, Batlló J, Matias L, Catita C, Jiménez MJ, García-Fernández M (2019) Maximum intensity maps (MIM) for Portugal mainland. *J Seismol* 23(3):417–440
- Volpe M, Lorito S, Selva J, Tonini R, Romano F, Brizuela B (2019) From regional to local SPTHA: efficient computation of probabilistic tsunami inundation maps addressing near-field sources. *Nat Hazards Earth Syst Sci* 19:455–469. <https://doi.org/10.5194/nhess-19-455-2019>
- Walley CD (1988) A braided strike-slip model for the northern continuation of the Dead Sea fault and its implications for Levantine tectonics. *Tectonophysics* 145:63–72
- Walley CD (1998) Some outstanding issues in the geology of Lebanon and their importance in the tectonic evolution of the Levantine region. *Tectonophysics* 298:37–62. [https://doi.org/10.1016/S0040-1951\(98\)00177-2](https://doi.org/10.1016/S0040-1951(98)00177-2)
- Wdowski Sh, Ben-Avraham Z, Arvidsson R, Ekstr`om G, (2006) Seismotectonics of the cyprian arc. *Geophys J Int* 164(1):176–181. <https://doi.org/10.1111/j.1365-246X.2005.02737.x>
- Wechsler N, Katz O, Dray Y, Gonen I, Marco S (2009) Estimating location and size of historical earthquake by combining archaeology and geology in Umm-El-Qanatir. *Dead Sea Transform Nat Hazards* 50:27–43

- Wechsler N, Rockwell TK, Klinger Y, Stepancikova P, Kanari M, Marco S, Agnon A (2014) A Paleoseismic record of earthquakes for the Dead Sea Transform fault between the first and seventh centuries CE: nonperiodic behavior of a plate boundary fault. *Bull Seismol Soc Am* 104:1329–1347
- Wetzler N, Segev A, Lyakhovsky V (2022) Uplift and subsidence at the periphery of the Lebanese Restraining Bend. *Tectonophysics, Northern Dead Sea Fault*. <https://doi.org/10.1016/j.tecto.2022.229292>
- Williams J (2023) 551 CE Beirut Earthquake, in *Earthquake Encyclopedia of the Dead Sea Transform - Pre-Instrumented Earthquakes felt or reported in the vicinity of the Dead Sea Transform*. <https://deads earthquake.info/EarthquakeCatalogOfTheDeadSea/551BeirutQuake.html#top> (Last Accessed July, 2023)
- Zohar M (2020) Temporal and spatial patterns of seismic activity associated with the dead sea transform (DST) during the Past 3000 Yr. *Seismol Res Lett* 91(1):207–221. <https://doi.org/10.1785/0220190124>
- Zohar M, Salamon A, Rubin E (2016) Reappraised list of historical earthquakes that affected Israel and its close surroundings. *J Seismol* 20(3):971–985
- Zucker E, Gvirtzman Z, Granjeon D, Garcia-Castellanos D, Enzel Y (2021) The accretion of the Levant continental shelf alongside the Nile Delta by immense margin-parallel sediment transport. *Mar Petrol Geol* 126:104876. <https://doi.org/10.1016/j.marpetgeo.2020.104876>
- Zviely D, Kit E, Klein M (2007) Longshore sand transport estimates along the Mediterranean coast of Israel in the Holocene. *Mar Geol* 238:61–73. <https://doi.org/10.1016/j.margeo.2006.12.003>

**Publisher's Note** Springer Nature remains neutral with regard to jurisdictional claims in published maps and institutional affiliations.

## Authors and Affiliations

Amos Salamon<sup>1,2,3</sup>  · Rachid Omira<sup>2,3</sup>  · Motti Zohar<sup>4</sup>  · Maria Ana Baptista<sup>3,5</sup> 

✉ Amos Salamon  
salamon@gsi.gov.il

Rachid Omira  
rachid.omira@ipma.pt

Motti Zohar  
motti.zohar@univ.haifa.ac.il

Maria Ana Baptista  
mavbaptista@gmail.com

<sup>1</sup> Geological Survey of Israel, Jerusalem, Israel

<sup>2</sup> Portuguese Institute for Sea and Atmosphere (IPMA), Lisboa, Portugal

<sup>3</sup> Instituto Dom Luiz – IDL, Faculdade de Ciências da Universidade de Lisboa, Lisboa, Portugal

<sup>4</sup> School of Environmental Science, University of Haifa, Haifa, Israel

<sup>5</sup> Instituto Superior de Engenharia de Lisboa, University of Lisbon, Lisboa, Portugal